Performance evaluation of EICP with organic/non-organic additives for repairing external cracks in cement-based materials

Jedrzejko, M. J.; Gan, Y.; Chen, X.; Jonkers, H. M.; Luo, H.

DOI
10.1016/j.conbuildmat.2024.139646

Publication date
2024

Document Version
Final published version

Published in
Construction and Building Materials

Citation (APA)
Jedrzejko, M. J., Gan, Y., Chen, X., Jonkers, H. M., & Luo, H. (2024). Performance evaluation of EICP with organic/non-organic additives for repairing external cracks in cement-based materials. *Construction and Building Materials*, *458*, Article 139646. https://doi.org/10.1016/j.conbuildmat.2024.139646

Construction and Building Materials 458 (2025) 139646

Contents lists available at ScienceDirect

Construction and Building Materials

journal homepage: www.elsevier.com/locate/conbuildmat

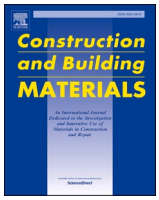

Performance evaluation of EICP with organic/non-organic additives for repairing external cracks in cement-based materials

M.J. Jedrzejko [a], Y. Gan [a,b,*], X. Chen [a,b], H.M. Jonkers [c], H. Luo [a,b]

[a] School of Civil and Hydraulic Engineering, Huazhong University of Science and Technology, Wuhan, 430074, China
[b] National Center of Technology Innovation for Digital Construction, Huazhong University of Science and Technology, Wuhan, 430074, China
[c] Microlab, Faculty of Civil Engineering and Geosciences, Delft University of Technology, Delft 2628 CN, the Netherlands

ARTICLE INFO

Keywords:
Crack repair
Enzyme-induced carbonate precipitation (EICP)
Microbially Induced calcium carbonate precipitation (MICP)
Calcium carbonate precipitation

ABSTRACT

This study compares Enzyme-Induced Calcium Carbonate Precipitation (EICP) and Microbially Induced Calcium Carbonate Precipitation (MICP) for repairing external cracks in cement-based materials. Cracks in cement-base members can compromise structural integrity and increase maintenance costs. Thus, cement-base specimens with controlled cracks were treated using EICPs and MICP, with organic and non-organic additives to enhance calcium carbonate formation. Results show that both methods were effective in sealing cracks smaller than 0.35 mm. While incorporated additives improved the overall precipitation effectiveness, influence the crystallite size and altern the morphology of precipitated calcium carbonate. MICP generated more consistent crystal structures, while EICPs resulted in diverse crystal shapes influenced by enzyme sources and additives. Both methods offer promising, sustainable solutions for crack repair, with EICP providing greater flexibility and easier preparation. Presented research gives the comprehensive insights into the field of crack repair via bio-based methods reveals its potential in this area.

1. Introduction

Cracking in concrete structures is an unavoidable consequence of the material's response to environmental and structural stresses. These cracks can develop due to a variety of factors, including thermal expansion, shrinkage, freeze-thaw cycles, chemical reactions such as alkali-silica reactions, and excessive or uneven load distribution. While some cracks may be superficial, without proper and regular maintenance, they can allow moisture to penetrate the concrete, leading to the corrosion of internal steel reinforcements, and even weakening of the overall structure [1–5]. Over time, cracks can significantly reduce the structure's lifespan, cause safety concerns, and increase repair costs. Hence, it is vital to address these issues early through timely repair and rehabilitation efforts, which help maintain the integrity, safety, and durability of the concrete structure [6–9].

Materials used for the repair of concrete cracks possess distinct properties, require varying levels of workforce expertise, and have different implications for structural performance, cost, and environmental impact [10,11]. Epoxy resins are known for their exceptional strength and bonding capabilities, making them ideal for structural crack repairs. However, their application demands highly qualified workers due to their complex handling, precise mixing ratios and application. Epoxy resins are costly and have a considerable environmental footprint because of their synthetic composition and energy-intensive production process [12,13]. Polyurethane sealants are flexible and water-resistant, suitable for non-structural cracks. Nevertheless, their reduced strength limits their use in load-bearing repairs, and like epoxy, their application requires trained workers [14,15]. Cement-based repair materials are more widely used due to their cost-effectiveness and ease of application. These materials are commonly applied by general laborers, though precision is needed for optimal performance. Structurally, cement-based grouts restore cracks well in static conditions, but they are less effective for dynamic cracks [16–18]. Environmentally, cement-based materials pose significant concerns due to the high carbon emissions associated with cement production. Cement manufacturing accounts for approximately 8 % of global CO_2 emissions, contributing heavily to climate change [19,20]. Silicone sealants offer excellent flexibility and moisture resistance but are limited in structural capacity and are therefore only suitable for surface-level, non-structural repairs.

The growing demand for sustainable and cost-effective methods to repair cracks in civil engineering structures has led researchers to

* Corresponding author at: School of Civil and Hydraulic Engineering, Huazhong University of Science and Technology, Wuhan 430074, China.
E-mail address: ygan@hust.edu.cn (Y. Gan).

https://doi.org/10.1016/j.conbuildmat.2024.139646
Received 12 November 2024; Received in revised form 15 December 2024; Accepted 17 December 2024

explore innovative alternatives to traditional materials. Among these, Microbially Induced Calcium Carbonate Precipitation (MICP) and Enzyme-Induced Carbonate Precipitation (EICP) have emerged as promising bio-mediated techniques that harness natural processes to enhance structural integrity.

MICP utilizes specific microorganisms, such as *Sporosarcina pasteurii*, to catalyze the precipitation of calcium carbonate ($CaCO_3$). These microbes initiate a series of biochemical reactions that convert urea into ammonium (NH_4^+) and carbonate ions (CO_3^{2-}). The carbonate ions then react with calcium ions (Ca^{2+}) in the environment, leading to the formation of calcium carbonate, which fills cracks and binds particles together. The core chemical reactions involved in MICP are [21–23]:

1. Urea hydrolysis (microbially catalyzed):

$$(NH_2)_2CO + H_2O \rightarrow 2NH_4^+ + CO_3^{2-} \quad (1)$$

2. Calcium carbonate precipitation:

$$Ca^{2+} + CO_3^{2-} \rightarrow CaCO_3 \quad (2)$$

Similarly, EICP employs the enzyme urease to induce the precipitation of calcium carbonate in cracks and pores. In EICP, the process begins with the urease-catalyzed hydrolysis of urea ($(NH_2)_2CO$), resulting in the production of ammonium (NH_4^+) and carbonate ions (CO_3^{2-}). These ions subsequently react with calcium ions, forming calcium carbonate precipitates that solidify the material.

The core chemical reactions involved in EICP are [24–26] similar to reactions (1) and (2) listed above. Both EICP and MICP offer bio-based solutions for repairing cracks in civil engineering structures, with the potential to improve durability and reduce the reliance on conventional materials.

Calcium carbonate precipitation process requires essential substrates such as urea, a calcium ion source (typically calcium chloride, $CaCl_2$), and urease. Urease can be sourced either from natural plant materials, such as jack beans and soybeans, or produced by bacteria or extracted commercially. Plant-derived urease is often considered more eco-friendly due to its renewable nature, but it may have lower enzymatic efficiency compared to industrially produced urease. Commercial urease, while more effective and consistent in large-scale applications, tends to be more expensive and may carry a greater environmental burden due to the manufacturing process [26–31]. In MICP, a similar set of substrates is required, including urea and a calcium ion source, but the urease enzyme is produced by specific microorganisms like *Sporosarcina pasteurii*. These microbes catalyze the same key reactions that lead to calcium carbonate precipitation. While MICP can be advantageous due to the self-sustaining nature of microbial activity, it requires careful control of microbial growth conditions and nutrient availability, which can be challenging in large-scale applications. By mimicking natural mineralization processes, both EICP and MICP offer more environmentally friendly alternatives to conventional concrete crack repair methods, reducing both carbon emissions and material costs albeit ammonia production might pose a concern in specific eutrophication-sensitive enviroments. EICP, with its use of plant-derived or commercially produced urease, is particularly noted for its adaptability and potential scalability, making it a promising solution in the pursuit of sustainable civil engineering practices.

Research into calcium carbonate precipitation techniques has explored both MICP and EICP as methods for stabilizing granular soils and controlling dust. EICP has shown significant potential, with studies successfully utilizing plant-derived urease from sources such as Glycine max (soybeans) and Canavalia ensiformis (jack beans) to stabilize loose sands and dust particles. For example, experiments using jack bean urease in EICP applications achieved substantial increases in soil strength, as evidenced by notable improvements in unconfined compression strength [31–34]. Similarly, plant-based urease has been effective in precipitating calcium carbonate within desert dust, reducing its erosion potential [35,36]. In parallel, MICP has been extensively studied for similar applications, relying on the metabolic processes of ureolytic bacteria like *Sporosarcina pasteurii* to induce calcite precipitation. Research has demonstrated that MICP can also significantly enhance soil strength and durability, particularly in sandy soils, through the bio cementation process [37,38]. While other studies have explored innovative strategies to optimize MICP for calcium carbonate precipitation, including understanding particle assembly and self-assembly mechanisms, enhancing control over bio-cementation processes, and developing magnetically responsive bacteria for targeted applications [39–41]. These advancements provide a foundation for improving efficiency, precision, and practicality in biomineralization techniques for engineering purposes. Furthermore, MICP was also employed for self-healing concrete, in which the bacteria and its nutrition were encapsulated and added to the concrete during the mixing process. When it comes to cracking of such concrete, the capsules also break releasing the encapsulated substrates which precipitated calcium carbonate after mixing [42–45].

Recent research on crack repair via MICP has shown promising results in crack repair. Jongvivatsakul [46] report that, the calcium carbonate (mostly vaterite) precipitated via MICP significantly reduced the crack width and also increase the material's strength and reduce the water absorption. Study presented in [47] evaluate the MICP effectiveness for crack repair in terms of nutrient concentration and low temperature. The repair was most successful for smaller cracks, although authors highlight challenges with uniform precipitation of calcium carbonate, especial for larger cracks. On the other hand, research presented in [48], highlighting that controlling bacterial and calcium ion concentrations had the most significant impact on repair outcomes, while environmental temperatures played a lesser role. Studies concerning crack repair using the EICP method, also highlighted its potential to effectively seal cracks and enhance the durability of cement-based materials. As reported in [49], the use of a biocementing suspension made from watermelon seed powder proved successful in healing cracks as wide as 0.5 mm within just seven days, demonstrating faster repair times compared to traditional methods. The treated mortar exhibited significant improvements in strength and durability, with decreased porosity and recovered compressive strength by up to 90 %. Another study [50] explored the incorporation of chitosan into the EICP process, which accelerated calcium precipitation and enhanced the efficiency of crack sealing. Chitosan also transformed calcium carbonate from metastable vaterite to stable calcite, leading to a more impermeable and durable repair. Field tests showed that chitosan-enhanced EICP could efficiently block cracks in tunnel linings, even in extreme environments, offering improved water resistance compared to traditional EICP. In a paper present by Li et al. [51], EICP was employed alongside quartz sand to fill cracks in concrete, achieving significant strength recovery and internal repair. The calcium carbonate formed within cracks was predominantly vaterite, and the process was shown to provide effective crack sealing, particularly in cracks ranging from 0.3 to 0.5 mm wide. Nevertheless, the repair efficiency depended on the number of treatment cycles, and future work suggested optimizing enzyme activity to reduce the time and effort required for large-scale applications.

However, the effectiveness of both EICP and MICP is influenced by factors such as the concentration of urease or bacterial activity, calcium ion availability, and environmental conditions. While MICP has proven successful, researchers have noted certain challenges, such as the need for cultivating and maintaining live bacteria, which can limit its applicability in certain environments. In contrast, EICP's use of plant-derived enzymes offers greater adaptability to a range of conditions, including oxygen-poor environments and lower temperatures, making it a versatile solution for enhancing the durability of structures and mitigating

crack propagation in challenging climates [31,52].

The conducted research mainly focuses on optimizing the precipitation process, treatment duration, and its overall impact on post-treatment performance. However, the interaction between the cement-based environment and calcium carbonate precipitation at the microscopic level remains underexplored. Furthermore, most research exclusively focuses on either the MICP or EICP method, which does not fully capture the potential of bio-related calcium carbonate precipitation methods for the repair of cracks in cement-based materials.

Therefore, this study presents a systematic research of calcium carbonate precipitation for cracks of cement base specimens via EICPs and MICP method. The main goal is to assess and compare the effectiveness/influence of organic and non-organic additives on these two approaches in repairing cracks within cement-based materials. By detailing the preparation of the specimens and the testing procedures, this research provides a thorough analysis of the calcium carbonate precipitation process. A 3D optical microscope is employed to capture the surface precipitation of the calcium carbonate within the cracks, while chemical and crystallographic analyses determine the types of calcium carbonate formed. Furthermore, the study examines the morphological differences between the EICP and MICP products, shedding light on their respective efficiencies in improving the structural integrity of cementitious materials.

2. Materials and experiment preparations

2.1. Preparation of cracked specimens

To evaluate calcium carbonate precipitation as a repair material, two types of cement-based specimens were used: cement paste (cement and water) and cement mortar (cement, sand, and water). Both specimen types had a water-to-cement ratio of 0.4, while the sand-to-cement ratio in the mortar specimens was 4:1. All specimens were cast on the same day in standard 70 × 70 × 70 mm molds and stored in a steam chamber for the first seven days, followed by 21 days under environmental conditions. After the curing period, the specimens were cut into four prisms, each approximately 32 × 32 × 70 mm in size, to reduce the specimen size and make them easier to handle, as shown in Fig. 1.

The prepared samples were then subjected to crack formation using a splitting test. Each specimen was placed in a compression machine, with a metal bar of 2 mm in diameter positioned on top. This bar served as a point of stress concentration, causing the specimen to crack as illustrated in Fig. 2. The load rate was set to the lowest possible value (i.e., 0.3 kN/s) on the testing machine, and loading was stopped as soon as a crack appeared on the specimen's surface. The maximum width of the cracks (directly under the metal bar) was 0.8 mm, and their length did not exceed 65 mm.

2.2. EICPs and MICP solutions

The key ingredient for the EICP method, urease, was extracted from two types of beans: Soy (*Glycine max*) and Jack (*Canavalia ensiformis*). The urease extraction followed these steps: (1) the dried beans were ground into a fine powder and sifted through a 0.2 mm mesh sieve; (2) the powder was mixed with deionized water at a ratio of 100 g per liter, stirred thoroughly for 30 minutes, and stored in the refrigerator at 4°C for over 12 hours; (3) the solution was centrifuged at 3000 rpm for 20 minutes; and (4) the urease extract was filtered and collected. For the MICP method, the gram-positive bacterium *Sporosarcina pasteurii* was selected due to its ability to precipitate calcium carbonate in the presence of urea and a calcium source. The bacteria were grown in an ammonium-yeast extract medium under laboratory conditions to achieve an optical density around OD600 = 0.8. The cementation solution, containing urea and a calcium ion source (calcium chloride anhydrous), those components was prepared with a molar concentration of 1 each for both repair methods. For the EICP method, the extracted urease was mixed with the cementation solution in a 1:1 ratio.

Fig. 1. Cement base specimens after demolding (left) and cut (right).

2.3. Specimens treatment

The cracked specimens were treated with the repair solutions through near-full immersion, as shown in Fig. 3. The upper portion of the samples was kept out of the repair solution to allow unrestricted access to oxygen, which is essential for the bacteria to function effectively in MICP solutions. This method was chosen to ensure an adequate supply of urea and calcium ions, promoting the precipitation of calcium carbonate crystals. The repair solutions were replaced with fresh solution every 12 hours. The total treatment time, or immersion duration, for the cracked specimens was 72 hours.

Additionally, the cementation solution was supplemented with an organic additive, low-fat milk powder, which has reportedly a beneficial effect on calcium carbonate precipitation. As reported by [53], casein in the milk powder provides extra nucleation sites and slows the precipitation rate, resulting in relatively larger crystals. The milk powder used in the present study consisted of about 45 % lactose, 35 % protein (mainly casein), less than 10 % of fat, and the remaining 10 % were minerals. While the chemical composition was as follow: chlorine (Cl) 36 %, titanium (Ti) 33 %, calcium (Ca) 17 %, potassium (K) 9 % and phosphorus (P) 5 %. Milk powder was added to the cementation solution at a ratio of 5 g per liter and thoroughly mixed until fully dissolved. This research also explores the effect of a non-organic additive in the form of concrete primer. Typically, concrete primer is applied to the surface of concrete before the application of materials like paint, sealants, or plaster to improve adhesion and prevent issues such as peeling, blistering, or efflorescence. In this study, the primer, which is hypothesized to also improve calcium carbonate precipitation through providing nucleation sites, and is an acrylic water-based polymer ($C_5H_8O_2$) containing surfactants, thickeners, and defoamers, contains elements such as carbon (C), hydrogen (H), oxygen (O) and also nitrogen (N) and sulfur (S). Primer was injected into selected specimens using a syringe a few hours before the EICPs and MICP treatments. Furthermore, some specimens were treated with a combination of milk powder in the cementation solution and primer application.

For the specimens treated with MICP, bacteria were injected into the cracks twice, with a 3-hour interval between applications. After 6 hours from the final bacteria injection, these samples were immersed in the cementation solution, following the procedure outlined above.

To facilitate identification and further analysis, each sample was given a specific nomenclature reflecting the treatment arrangements for EICPs and MICP. The first part of the name corresponds to the treatment type (E – EICP; S – Soy bean urease; J – Jack bean urease; M – MICP), followed by letters indicating organic or non-organic additives (0 – none; M – milk powder; P – primer; MP – milk powder and primer). The final part of the specimen names refers to the material type (P – cement paste; M – cement mortar). For instance, EJ-MP-M refers to EICP treatment using urease extracted from Jack beans, with the cracks treated with primer and a cementation solution containing milk powder the

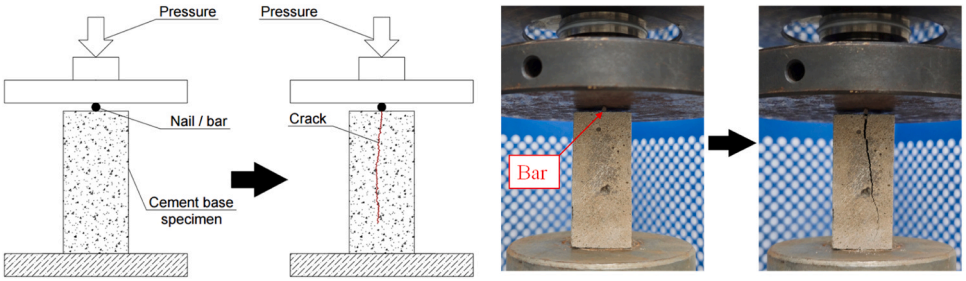

Fig. 2. Crack manufacturing.

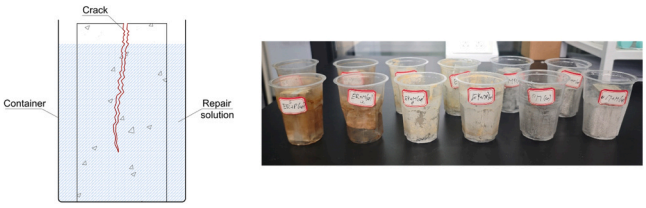

Fig. 3. Immersion of cracked specimens in repair solution.

specimen, while M-M-P refers to MICP treatment with the addition of milk powder in the cementation solution for cement paste specimens. Table 1 provides a detailed summary of all specimens and their treatments.

3. TESTs program

3.1. Optical 3D microscope surface analyses

All external cracked surfaces of the specimens were analyzed using a 3D optical microscope (Aosvi 3D-HD228S). Microscopic analyses were performed before the EICPs/MICP treatments, with images taken every 24 hours throughout the treatment period. This analysis enabled precise measurement of crack widths and allowed visual monitoring of calcium carbonate precipitation on the crack surfaces between immersion stages. To ensure accurate tracking of the healing process, each specimen's crack was marked with six distinct spots on both sides (three per side). These positions were numbered from 1 to 6, corresponding to similar locations: near the crack tip (lower end), the middle, and close to the loading point (i.e., under the metal bar). Fig. 4 illustrates the concept of crack measurement, and Table 1 provides detailed information regarding the crack widths.

3.2. Chemical and crystallography analyses

After the treatments were completed, the products of EICPs and MICP were further examined for their chemical composition using X-ray fluorescence (XRF) analysis. XRF is a powerful analytical technique that determines the chemical composition of materials by measuring the characteristic X-rays emitted from a sample when excited by a primary X-ray source. These emitted X-rays are unique to each element, enabling both qualitative and quantitative analysis of the elements present in the sample. Samples for XRF analysis were carefully prepared by collecting (scraping) compounds from the surface of the cracks and drying them for several hours. The dried material was then finely ground in a mortar to achieve a homogeneous powder, which was passed through a 200-mesh sieve to obtain particles approximately 74 μm in size. These prepared samples were subsequently subjected to XRF analysis.

X-ray diffraction (XRD) is a fundamental technique used to analyze the crystallographic structure of materials. By directing X-rays at a crystalline sample, XRD measures the diffraction patterns produced as the rays interact with the periodic arrangement of atoms. These patterns provide detailed information about the crystal structure, including

Table 1
Specimens' details.

Name	Treatment	Additives	Specimens type	Cracks width [mm]					
				1	2	3	4	5	6
EJ−0-P	EICP –	None	Cement paste	0.25	0.22	0.12	0.11	0.20	0.31
EJ-M-P	Jack beans urease	Milk powder		0.19	0.22	0.21	0.12	0.08	0.71
EJ-P-P		Primer		0.15	0.12	0.11	0.15	0.17	0.20
EJ-MP-P		Milk + primer		0.18	0.15	0.12	0.25	0.31	0.37
EJ−0-M	EICP –	None	Cement mortar	0.15	0.27	0.35	0.46	0.32	0.18
EJ-M-M	Jack beans urease	Milk powder		0.21	0.39	0.63	0.53	0.45	0.22
EJ-P-M		Primer		0.11	0.26	0.29	0.31	0.22	0.16
EJ-MP-M		Milk + primer		0.13	0.21	0.32	0.35	0.29	0.15
ES−0-P	EICP –	None	Cement paste	0.20	0.14	0.11	0.12	0.21	0.22
ES-M-P	Soy beans urease	Milk powder		0.11	0.12	0.09	0.08	0.10	0.09
ES-P-P		Primer		0.12	0.09	0.08	0.11	0.11	0.13
ES-MP-P		Milk + primer		0.26	0.23	0.17	0.12	0.26	0.20
ES−0-M	EICP –	None	Cement mortar	0.22	0.25	0.37	0.36	0.23	0.14
ES-M-M	Soy beans urease	Milk powder		0.20	0.38	0.70	0.40	0.31	0.24
ES-P-M		Primer		0.19	0.31	0.43	0.39	0.29	0.21
ES-MP-M		Milk + primer		0.12	0.31	0.52	0.52	0.33	0.21
M−0-P	MICP	None	Cement paste	0.44	0.38	0.20	0.24	0.29	0.69
M-M-P		Milk powder		0.18	0.17	0.14	0.10	0.19	0.23
M-P-P		Primer		0.19	0.24	0.34	0.29	0.18	0.12
M-MP-P		Milk + primer		0.15	0.12	0.11	0.15	0.12	0.13
M−0-M	MICP	None	Cement mortar	0.11	0.27	0.52	0.51	0.38	0.22
M-M-M		Milk powder		0.18	0.30	0.69	0.67	0.51	0.25
M-P-M		Primer		0.19	0.25	0.40	0.42	0.32	0.17
M-MP-M		Milk + primer		0.10	0.20	0.32	0.28	0.20	0.11

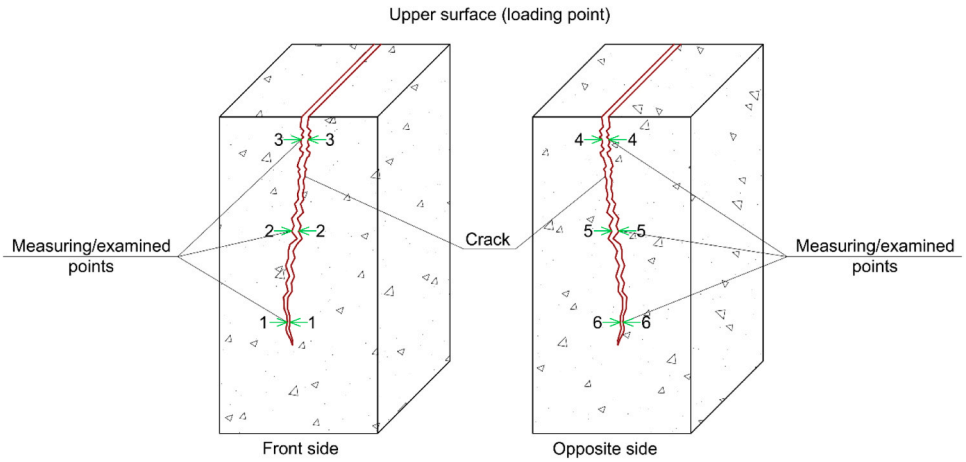

Fig. 4. Schematic view of points subjected to microscopic analyzes.

lattice parameters, phase identification, and atomic spacing. XRD is essential for determining the crystallinity and phase composition of EICPs and MICP products. A similar procedure was followed for XRD analysis, with powders of EICPs and MICP products collected from the opposite side of the crack. In this case, the powders were sieved through a 300-mesh sieve, yielding particles approximately 50 μm in size.

3.3. Morphology analyses

Scanning Electron Microscopy (SEM) was used for morphology analysis, providing detailed imaging of the material's surface structure and texture at the micro- to nanometer scale. SEM operates by scanning a focused beam of electrons across the sample surface, generating high-resolution images that reveal topographical details such as grain size, particle shape, surface roughness, and porosity. When combined with Energy-Dispersive X-ray Spectroscopy (EDS), SEM can also provide atomic compositional information.

Samples for SEM analysis were carefully selected to obtain the best possible images. To achieve this, calcium carbonate crystals were cut from the inner plane of the cracks into small pieces, with a base material thickness of 2–3 mm. These samples were then gently cleaned in water and dried in an oven overnight. Afterward, a necessary coating was applied before subjecting them to SEM analysis

4. Results and discussion

This section presents and compiles the results of the aforementioned analysis conducted for EICPs and MICPs techniques used in cement-based materials.

4.1. Calcium carbonate precipitation on the crack surface – microscopic analyses

Cracked surface of cement-based material (cement paste and mortar) were analyzed in detail under the 3D optical microscope in order to evaluate the calcium carbonate precipitation over the time. The following sections present images of the samples before and after the full period of planned treatment for the cracks below and above 0.35 mm. Additionally, photos of the specimens after treatment include the percentage coverage of the crack surface by precipitated calcium carbonate. Crack coverage was estimated through image processing of the samples' photographs taken before and after the complete treatment. Detailed summary of calcium carbonate precipitation images taken every 12 hours are included in Appendix A.

4.1.1. Cement paste specimens

Analyzing Figs. 5–7, formation of calcium carbonate precipitation on the surface of the crack, as well as in its inner plane, can be clearly seen. Crack filling efficiency significantly depends on the crack's width. In general, regardless of the method (EICP as well as MICP), cracks less than 0.35 mm wide were markedly filled with calcium carbonate. The confined space in these narrower cracks promotes crystal nucleation and growth, allowing nearly full coverage of the crack surface, with calcium carbonate filling percentages ranging from 96.82 % to 100 %. For cracks wider than 0.35 mm, however, calcium carbonate was deposited only partially, with crack coverage percentages ranging from 45.58 % to 79.64 % (except EJ-MP-P specimen which is 11.56 %). The influence of additives, such as milk powder and primer, in these wider cracks was marginal, with only slight variations in coverage observed. This suggests that while additives may enhance crack sealing in narrower cracks, they do not significantly improve the performance in wider cracks. Furthermore, in cracks wider than 0.35 mm, the larger voids make it more difficult for the crystals to coalesce and fully seal the crack, leading to incomplete or absent precipitation. Additionally, the reduced surface area for crystal attachment in wider cracks further hinders the process.

4.1.2. Cement mortar specimens

Building on the findings from cement paste specimens, similar trends were observed in the cement mortar samples regarding calcium carbonate precipitation, as seen in Figs. 8–10. However, the presence of sand in cement mortar introduces additional complexity. The sand particles not only create a more porous structure but also contribute to larger, irregularly shaped voids and a more heterogeneous surface. These factors affect how calcium carbonate crystals form and attach within the cracks. In cracks narrower than 0.35 mm, the confined space between sand grains aids in crystal nucleation and growth, much like in the cement paste. As a result, these cracks still exhibit significant filling with the 100 % coverage for EICPs treated specimens. However, the percentage coverage of crack surface for specimens treated with MICP ranging from 80.12 % to 100 % (except specimen M-M-M). In contrast, for cracks wider than 0.35 mm, the combination of a coarser texture and increased porosity makes it more challenging for the repair solutions to distribute evenly and for calcium carbonate to form a continuous deposit. The irregular surfaces and larger voids mean that calcium carbonate crystals struggle to coalesce effectively, leading to partial or absent filling. The crack coverage in these wider cracks ranged from 15.56 % to 83.21 %, depending on the treatment. Additionally, the presence of additives like milk powder and primer had only a marginal effect on the filling efficiency in these wider cracks. While there was some variation in coverage, the overall challenge of distributing the repair material evenly and forming a cohesive deposit remained

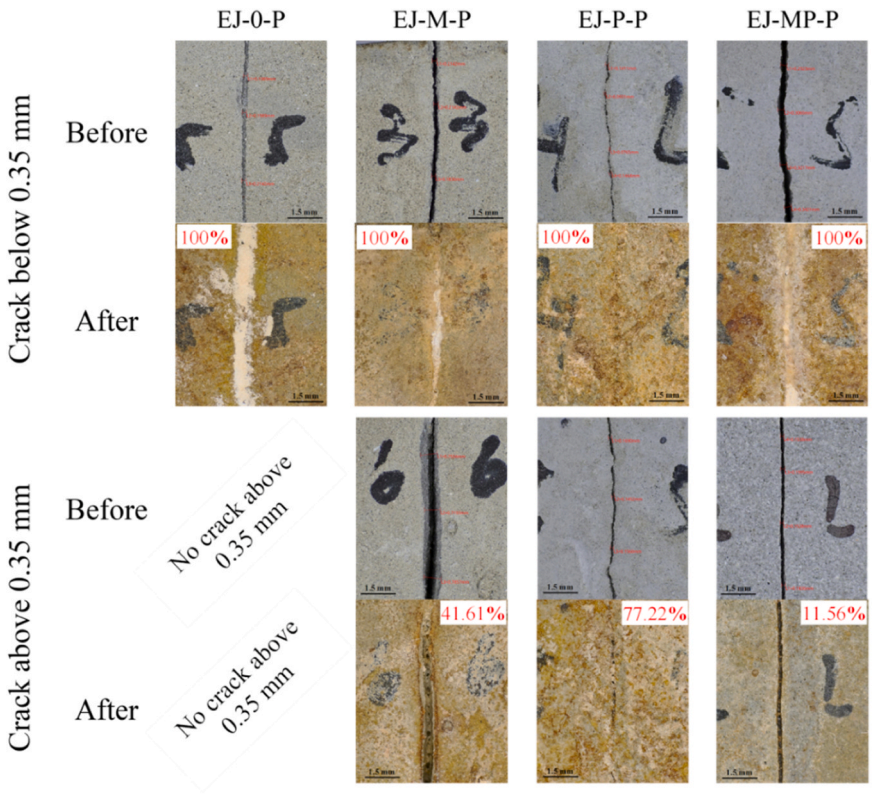

Fig. 5. Cracks surface of cement paste specimens before and after EICP(J) treatment.

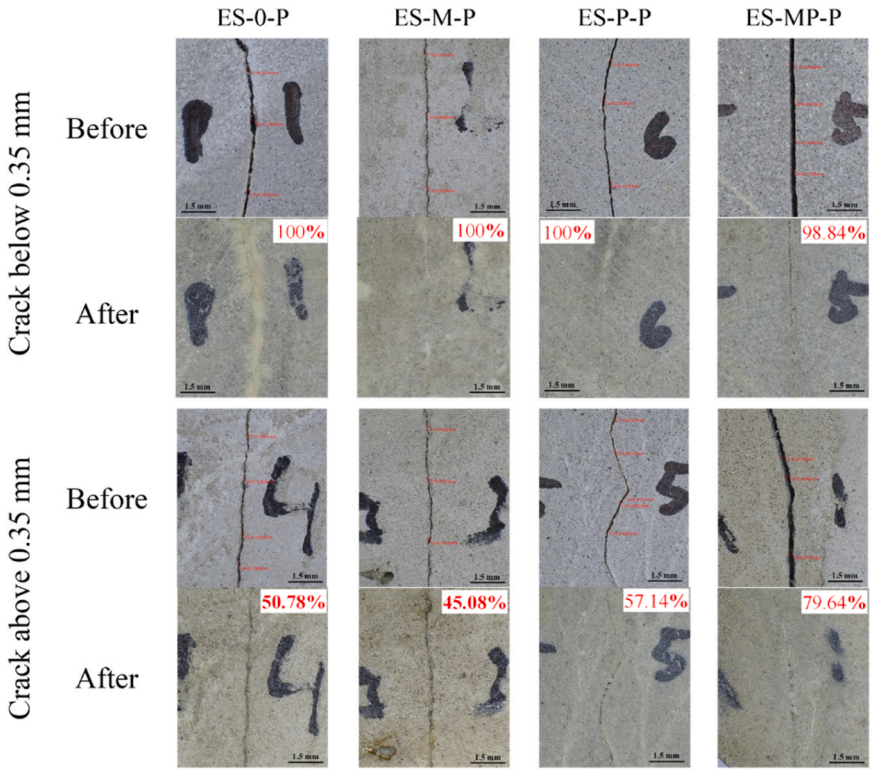

Fig. 6. Cracks surface of cement paste specimens before and after EICP(S) treatment.

significant. These structural differences in mortar, including fewer suitable nucleation sites compared to cement paste, limit the ability of calcium carbonate to bridge gaps in wider cracks, resulting in less effective crack healing.

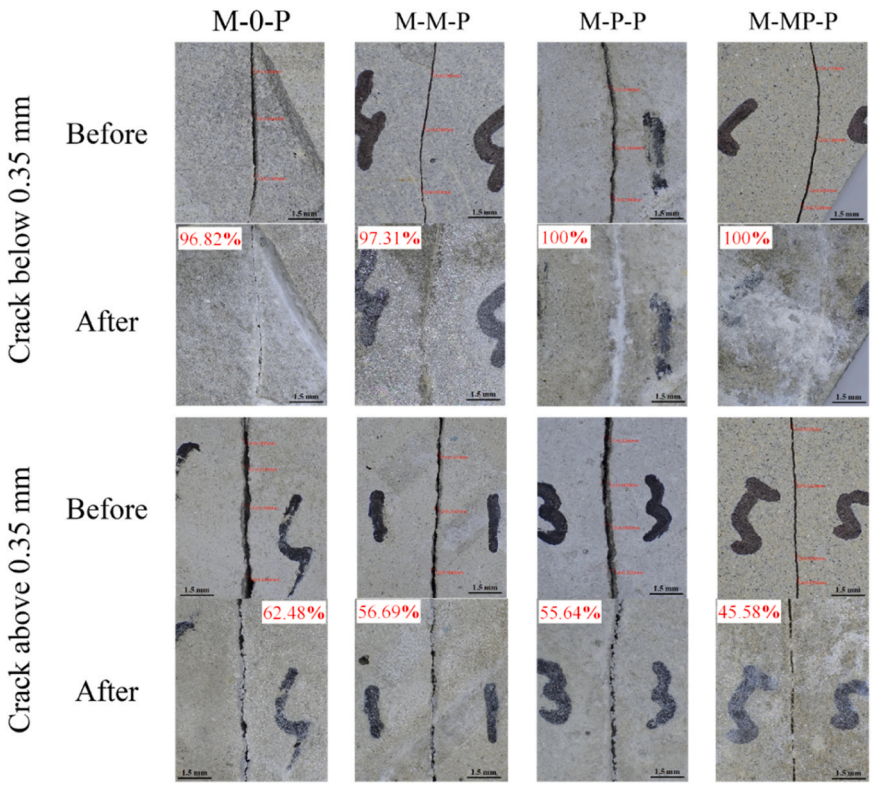

Fig. 7. Cracks surface of cement paste specimens before and after MICP treatment.

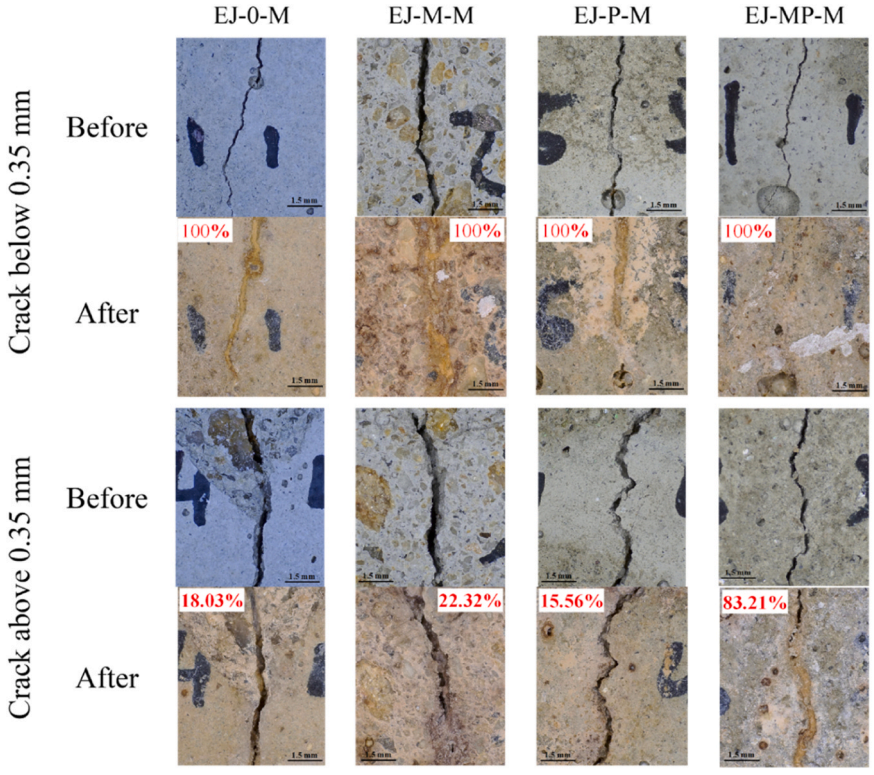

Fig. 8. Cracks surface of cement mortar specimens before and after EICP(J) treatment.

4.2. Chemical composition and crystallography – XRF and XRD outcomes

4.2.1. Results of XRF analyses – chemical composition

Table 2 presented the XRF data of precipitated minerals, for the various treatments (i.e., EICPs and MICP with different additives). This analysis focuses on the elemental compositions in terms of weight percentage (n.wt.), atomic percentage (n.at.) and error margins for n.wt. (Error).

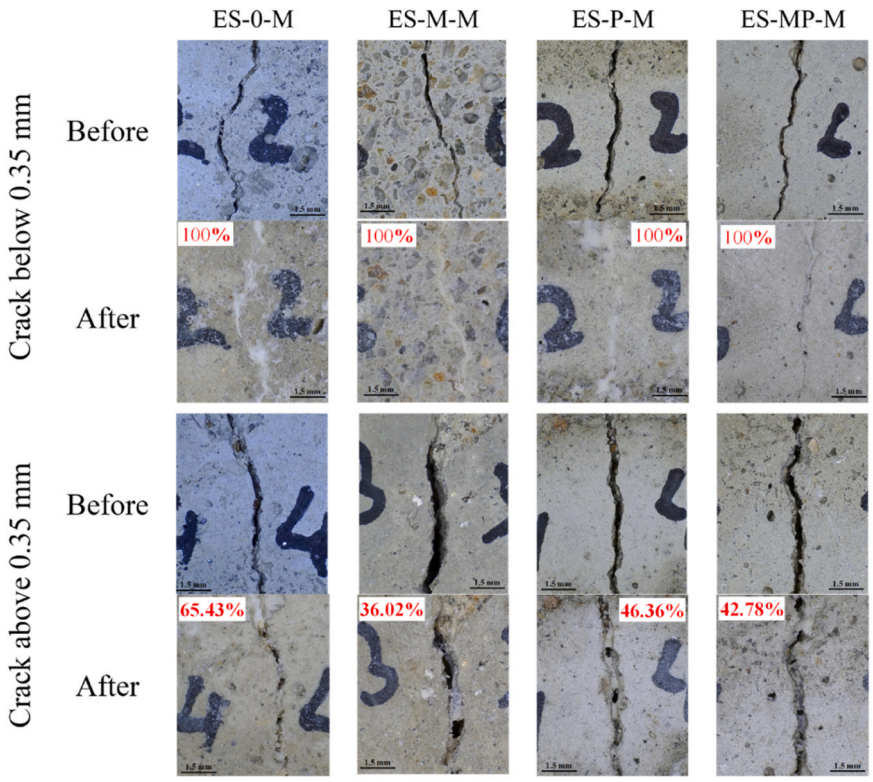

Fig. 9. Cracks surface of cement mortar specimens before and after EICP(S) treatment.

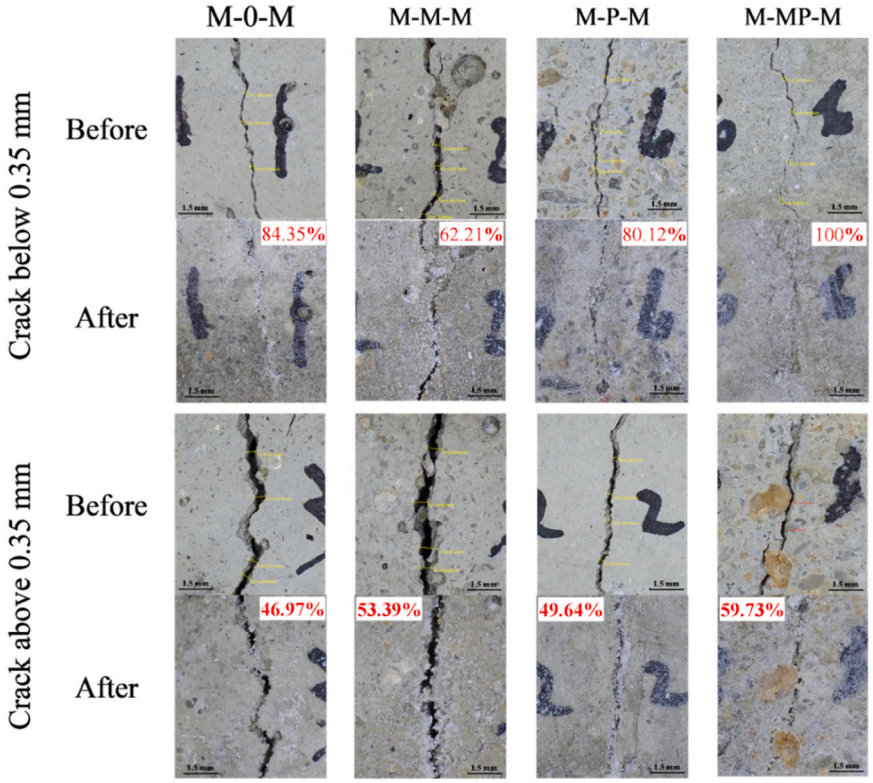

Fig. 10. Cracks surface of cement mortar specimens before and after MICP treatment.

The dominant component across all treatments is calcium (Ca), reflecting the primary role of calcium carbonate in both EICPs and MICP processes. In EICPs treatments, calcium content shows more variation, ranging from 60.56 wt% to 79.26 wt%. The lower calcium concentrations observed in some EICP treatments, such as EICP (J) + milk, with 60.56 wt% Ca, suggest that the process may yield more complex

Table 2
X-ray fluorescence results of EICPs and MICP products.

Element Treatment		Al	Ca	Cl	Fe	Mg	Mn	P	K	Si	Sr	S	Ti
EICP (J)	n.wt. [%]	1.08	**64.51**	20.7	2.97	-	0.07	1.75	2.19	5.85	-	0.67	0.16
	n.at. [%]	1.51	**61.11**	22.20	2.02	-	0.05	2.15	2.13	7.90	-	0.79	0.12
	Error [%]	0.037	0.091	0.068	0.011	-	0.002	0.024	0.022	0.056	-	0.012	0.005
EICP (J) + milk	n.wt. [%]	0.59	**60.56**	32.84	0.61	-	0.04	1.29	1.07	2.12	0.08	0.66	0.13
	n.at. [%]	0.82	**57.24**	35.09	0.41	-	0.03	1.58	1.04	2.86	0.03	0.78	0.10
	Error [%]	0.009	0.032	0.030	0.002	-	0.001	0.007	0.006	0.012	0.001	0.004	0.001
EICP (J) + primer	n.wt. [%]	1.55	**79.26**	3.71	2.74	-	0.09	0.98	2.06	8.43	0.17	0.72	0.21
	n.at. [%]	2.20	**75.91**	4.02	1.88	-	0.06	1.23	2.02	11.52	0.07	0.87	0.16
	Error [%]	0.015	0.031	0.009	0.004		0.001	0.006	0.006	0.022	0.001	0.004	0.001
EICP (J) + milk, primer	n.wt. [%]	1.63	**74.95**	3.83	2.55	0.28	0.10	2.34	6.37	5.74	0.11	1.62	0.34
	n.at. [%]	2.33	**71.88**	4.15	1.75	0.44	0.07	2.91	6.26	7.85	0.05	1.95	0.27
	Error [%]	0.015	0.030	0.009	0.004	0.012	0.001	0.009	0.010	0.018	0.001	0.006	0.002
EICP (S)	n.wt. [%]	0.10	**89.03**	7.50	0.03	-	0.02	1.59	1.07	0.09	0.07	0.51	-
	n.at. [%]	0.15	**87.60**	8.34	0.02	-	0.01	2.02	1.08	0.12	0.04	0.63	-
	Error [%]	0.004	0.037	0.014	0.001	-	0.001	0.008	0.005	0.003	0.001	0.004	-
EICP (s) + milk	n.wt. [%]	-	**92.37**	5.64	0.03	0.26	0.01	0.39	0.82	0.03	0.07	0.38	-
	n.at. [%]	-	**91.37**	6.30	0.02	0.43	0.01	0.50	0.83	0.04	0.03	0.47	-
	Error [%]	-	0.037	0.012	0.001	0.013	0.001	0.004	0.004	0.001	0.00	0.003	-
EICP (S) + primer	n.wt. [%]	0.10	**91.57**	4.42	0.01	0.02	0.02	0.47	0.78	2.14	0.06	0.33	-
	n.at. [%]	0.14	**90.02**	4.91	0.07	0.03	0.11	0.60	0.79	3.00	0.03	0.41	-
	Error [%]	0.004	0.034	0.010	0.001	0.003	0.001	0.004	0.004	0.012	0.001	0.003	-
EICP (S) + milk, primer	n.wt. [%]	0.01	**89.01**	9.30	0.01	0.16	-	0.20	0.84	-	0.09	0.46	-
	n.at. [%]	0.02	**87.74**	10.36	0.01	0.26	-	0.25	0.85	-	0.04	0.46	-
	Error [%]	0.001	0.034	0.014	0.001	0.009	-	0.003	0.004	-	0.001	0.003	-
MICP	n.wt. [%]	0.05	**96.16**	1.40	0.26	-	-	0.05	0.10	0.06	0.04	0.36	-
	n.at. [%]	0.08	**95.79**	2.31	0.43	-	-	0.08	1.17	0.09	0.06	0.60	-
	Error [%]	0.004	0.034	0.007	0.002	-	-	0.002	0.002	0.002	0.001	0.004	-
MICP + milk	n.wt. [%]	-	**96.80**	2.45	0.02	-	-	0.09	-	-	0.03	0.55	0.06
	n.at. [%]	-	**96.37**	2.76	0.02	-	-	0.12	-	-	0.02	0.68	0.05
	Error [%]	-	0.034	0.007	0.001	-	-	0.002	-	-	0.001	0.003	0.001
MICP + primer	n.wt. [%]	-	**94.01**	5.33	-	-	-	0.03	-	0.18	0.03	0.43	-
	n.at. [%]	-	**93.19**	5.98	-	-	-	0.03	-	0.25	0.13	0.53	-
	Error [%]	-	0.036	0.011	-	-	-	0.001	-	0.004	0.001	0.003	-
MICP + milk, primer	n.wt. [%]	0.16	**97.79**	0.48	0.12	-	0.02	0.21	0.10	0.33	0.04	0.66	0.08
	n.at. [%]	0.24	**97.37**	0.55	0.08	-	0.02	0.27	0.1	0.47	0.02	0.82	0.07
	Error [%]	0.005	0.033	0.003	0.001	-	0.001	0.003	0.001	0.004	0.001	0.003	0.001

Note: n.wt. = Normalized weight; n.at. = normalized atomic weight; Error = error of n.wt.

precipitates, potentially incorporating other elements. This is supported by the higher chlorine (Cl) content, which reaches 32.84 wt% in EICP (J) + milk, indicating possible involvement of chloride salts in the precipitates, as the chlorine is one of the main elements of used milk powder. Sulfur (S), although present in small quantities, is more consistently observed across treatments, particularly in EICP mixtures. Its presence might be attributed to residual sulfate used in the process or sulfate-bearing compounds precipitating alongside calcium carbonate. Notably, sulfur reaches 1.62 wt% in EICP (J) + milk, primer treatment, suggesting some variation in sulfate incorporation depending on the treatment conditions. Chlorine (Cl) levels are also significant in the EICP treatments, notably in the EICP (J) + milk sample, where it comprises 32.84 wt%. When comparing the MICP treatments, calcium content remains notably high, exceeding 94 wt%, particularly in the MICP with milk and primer treatment, where calcium reaches 97.79 wt%. This is consistent with the expected calcium carbonate precipitation, as MICP primarily functions by promoting $CaCO_3$ formation. The minimal presence of other elements, such as iron (Fe) and aluminum (Al), confirms the purity of the calcium carbonate precipitates formed in these MICP treatments. Furthermore, increase in Cl content, relative to MICP, could indicate the presence of additional chlorinated compounds, which are potentially incorporated into the mineral matrix or in case of EICPs, they are residues from the enzyme solutions and supplementations of milk powder. Moreover, silicon (Si) and potassium (K), which are typically found in soil or environmental materials, appear at low levels in both EICPs and MICP treatments. Their presence could result from minor contamination or some base materials (cement) were also scratch during the collecting of EICPs and MICP products from the specimens.

In summary, the XRF analysis highlights that calcium dominates the composition of both EICPs and MICP precipitates, as expected due to the calcium carbonate focus of both treatments. However, the EICP treatments show a broader elemental variety, including higher Cl and P contents, indicating a more complex mineralogy. The variations across treatments—particularly the addition of milk and primer—suggest a nuanced influence of these additives on the mineral composition, with notable shifts in Cl, S, and Si levels.

4.2.2. *Results of XRD analyses – crystallography*

The results of XRD test analyses after processing the data properly are shown in Figs. 11–13 for the EICP(J), EICP(S) and MICP methods, respectively. The XRD analysis conclusively identified calcium

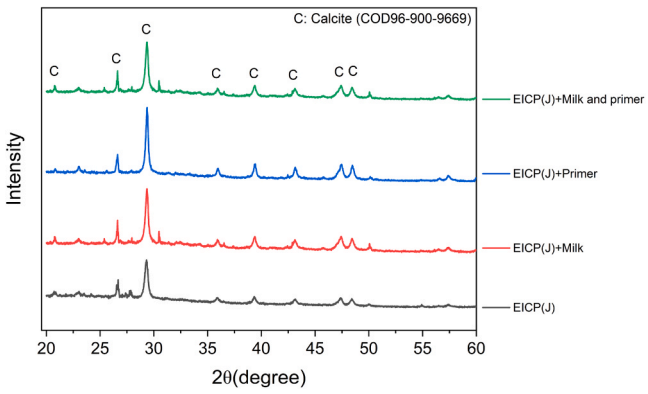

Fig. 11. XRD analyses outcome of EICP(J)s' products.

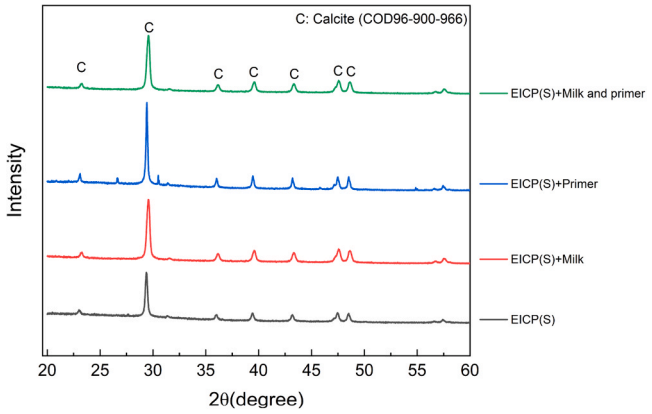

Fig. 12. XRD analyses outcome of EICP(S)s' products.

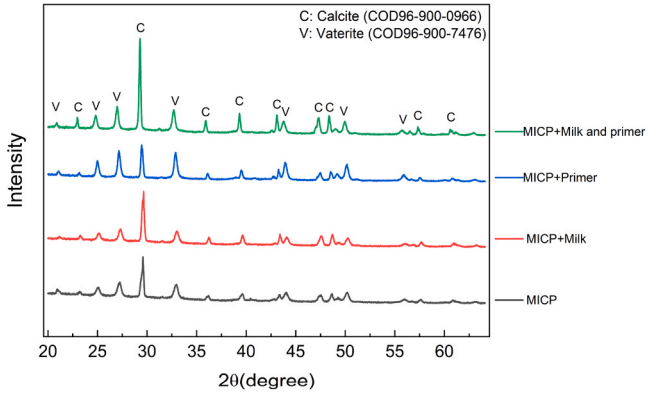

Fig. 13. XRD analyses outcome of MICPs' products.

carbonate as the dominant phase in EICPs and MICP-treated samples, with distinct diffraction peaks corresponding to calcite, the most thermodynamically stable form of calcium carbonate. Furthermore, in the MICP-treated samples, vaterite, a less stable polymorph of calcium carbonate, was also detected. The presence of calcite and vaterite across both methods indicates their effectiveness in promoting the crystallization of calcium carbonate, despite differences in the underlying precipitation mechanisms. Worthnoted, while the same phase was obtained, the relative peak intensities showed slight variations between the two methods. This suggests potential differences in crystal size, orientation, or even crystallinity, with the EICPs-treated samples possibly exhibiting more uniform or densely packed crystals compared to those formed through MICP. These subtle distinctions could be linked to the more controlled, biologically mediated precipitation in MICP, where microbial activity may offer a more favourable environment for the nucleation and growth of calcite crystals. In contrast, the enzyme-driven (EICP) process, while still producing calcite, might result in more irregular morphology of crystal formation. These differences warrant further investigation, such as mechanical testing, to determine how the crystal structure might impact the durability, strength, or long-term stability of the treated cementitious materials.

The XRD analysis not only identifies the types of calcium carbonate crystals formed during the healing and sealing process in cement-based materials but also reveals variations in crystallite size (Table 3), which significantly influence crack repair efficiency. For MICP, the crystallite size increases substantially with the addition of milk powder and primer, with the largest size reaching 66.25 nm when both additives are used, compared to 33.12 nm for pure MICP. This growth in crystallite size suggests enhanced crack healing potential, as larger and more cohesive calcium carbonate structures form within the cracks. In addition to

Table 3
Crystallite size of calcium carbonate for different variations of MICP and EICPs.

	Calcium carbonate products precipitated via different solutions			
	MICP	MICP + Milk	MICP + Primer	MICP + Milk and primer
Crystallite size [nm]	33.12	40.54	44.24	66.25
	EICP (J)	EICP(J)+ Milk	EICP(J)+ Primer	EICP(J) + Milk and primer
Crystallite size [nm]	38.72	44.62	57.74	44.77
	EICP (S)	EICP(S)+ Milk	EICP(S)+ Primer	EICP(S) + Milk and primer
Crystallite size [nm]	22.38	26.70	29.22	24.25

crystallite size, the XRD results highlight distinct differences in the proportion of calcite and vaterite formed under various MICP treatments. Conventional MICP yielded 43 % calcite and 57 % vaterite. When milk powder was introduced, calcite content increased dramatically to 81 %, with vaterite reducing to 19 %. In contrast, the use of primer alone resulted in a shift towards 38 % calcite and 62 % vaterite. The combination of milk powder and primer produced a balanced outcome, with 49 % calcite and 51 % vaterite. These variations underscore how additives influence the mineralogical composition of the precipitated calcium carbonate. Milk powder appears to favor the formation of calcite, a more stable and cohesive polymorph, while primer tends to promote a higher proportion of vaterite. Their combined use creates a balanced crystal distribution, potentially optimizing the material's healing performance by leveraging the unique properties of both polymorphs. In case of plant urease treatments, the EICP(J) shows a notable increase in crystallite size with primer (57.74 nm), potentially improving crack sealing properties. In contrast, the EICP(S) method produces generally smaller crystallites, with the largest size of 29.22 nm observed with primer. These variations in crystallite size suggest that the additives and their effects on calcium carbonate precipitation could be tailored to optimize crack healing performance in different cement-based materials.

4.3. *Morphology – SEM outcome*

The SEM micrographs presented in Figs. 14–19 showcase the morphology of calcium carbonate precipitates produced through MICP and EICPs within cracks of cement paste and mortar specimens. The crystallization and overall structure of the calcium carbonate deposits vary depending on the additives and treatment conditions, displaying distinct characteristics across the different groups. The MICP morphology is analyzed first, since this method is already well known and will serve as a kind of comparison.

4.3.1. *Calcium carbonate in cement paste specimens*

In the conventional MICP-treated specimens, where no additives were employed, calcium carbonate primarily formed as spherical and rhombohedral crystals (Fig. 14a). The spherical crystals are indicative of the vaterite polymorph, while the rhombohedral shapes correspond to calcite. These formations are relatively isolated and sparsely distributed across the crack surfaces, possibly leading to minimal crack coverage and, consequently, limited healing efficacy. When milk powder is introduced, the crystal morphology undergoes significant changes, resulting in the formation of elongated, needle-like calcite crystals (Fig. 14b). These crystals are more densely packed and creating a slightly better cohesive structure. The intricate and interlocking nature of these crystals suggests an enhanced capacity for crack filling compared to the conventional MICP treatment. Additionally, the presence of rod-like triangular patterns suggests that organic compounds in the milk powder promote crystallization and enhance the formation of well-defined crystal structures. In specimens where a primer was applied

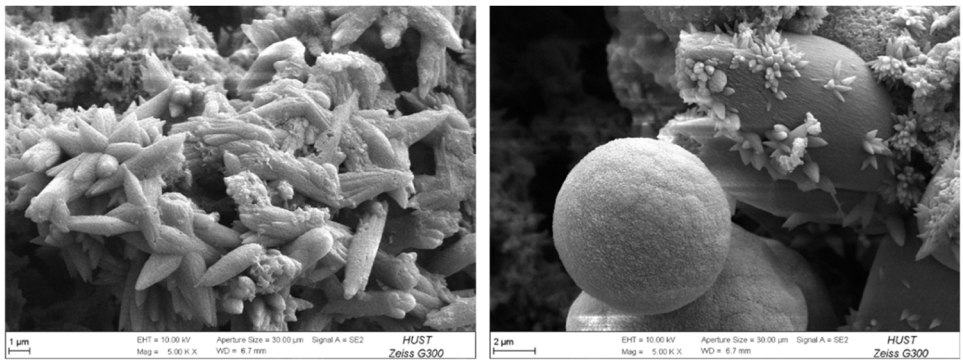

a) MICP

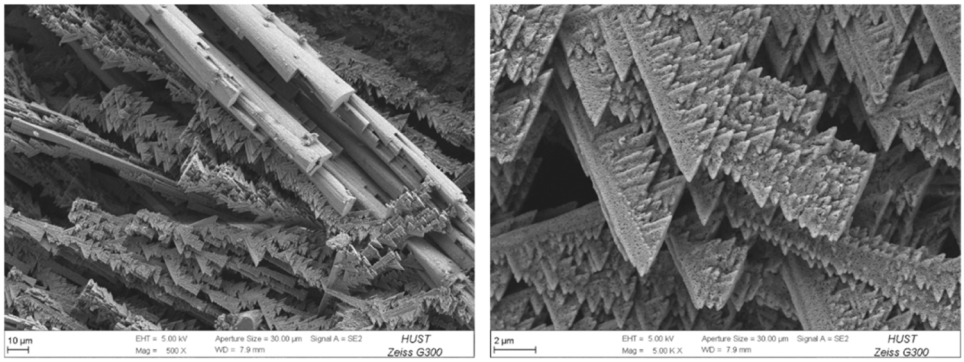

b) MICP + Milk powder

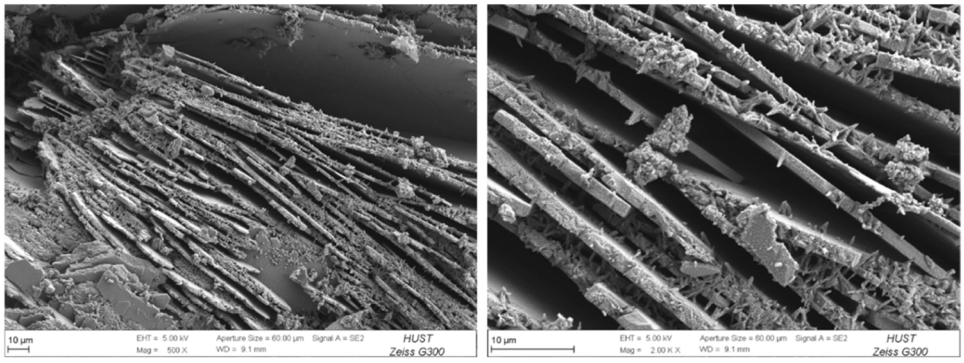

c) MICP + Primer

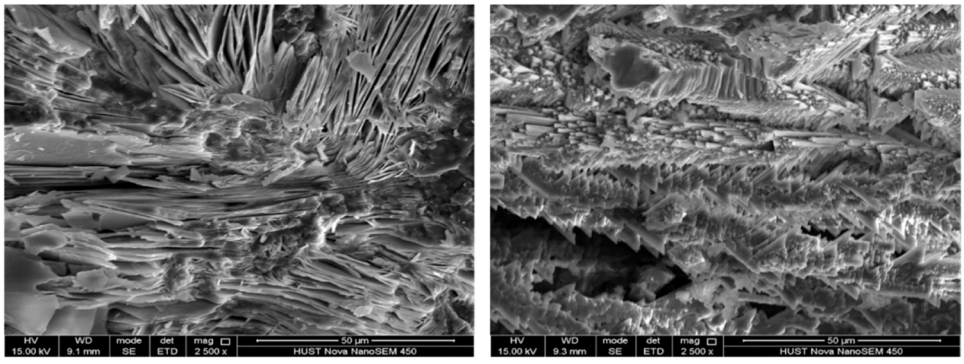

d) MICP + Milk powder and primer

Fig. 14. SEM analyses outcome of MICPs' products in cement paste specimens.

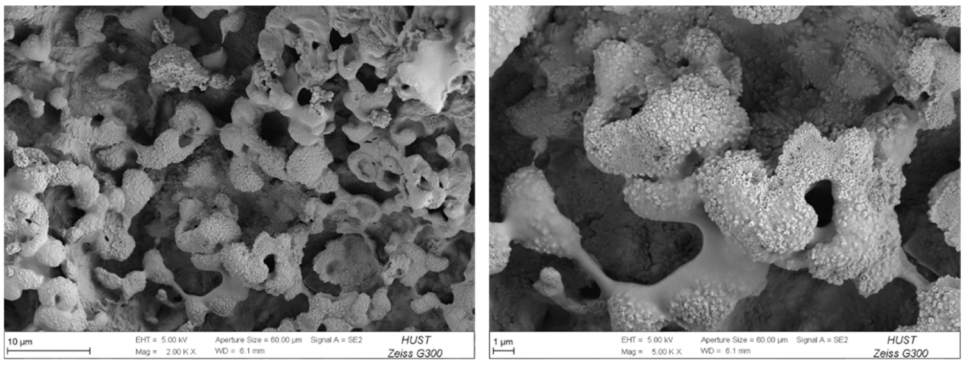

a) EICP(J)

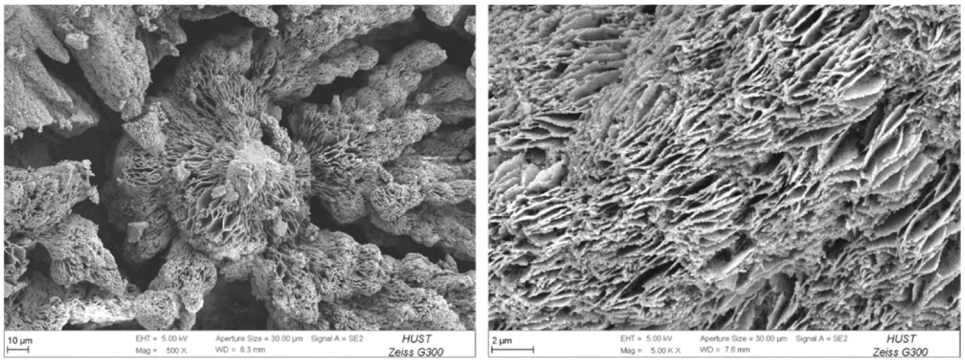

b) EICP(J) + Milk powder

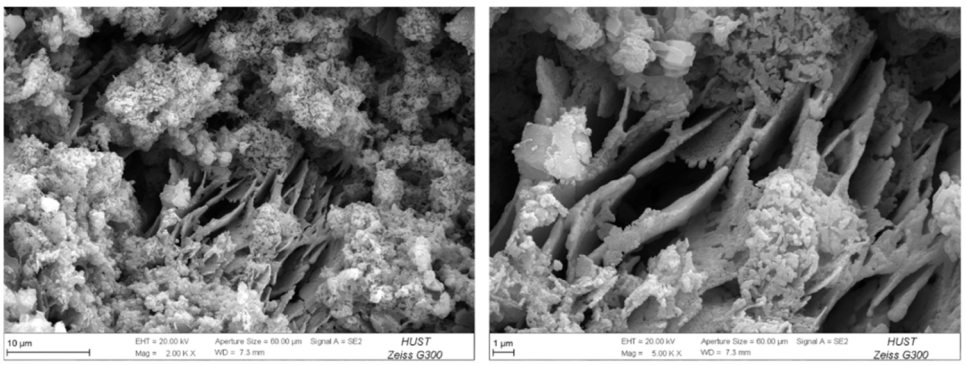

c) EICP(J) + Primer

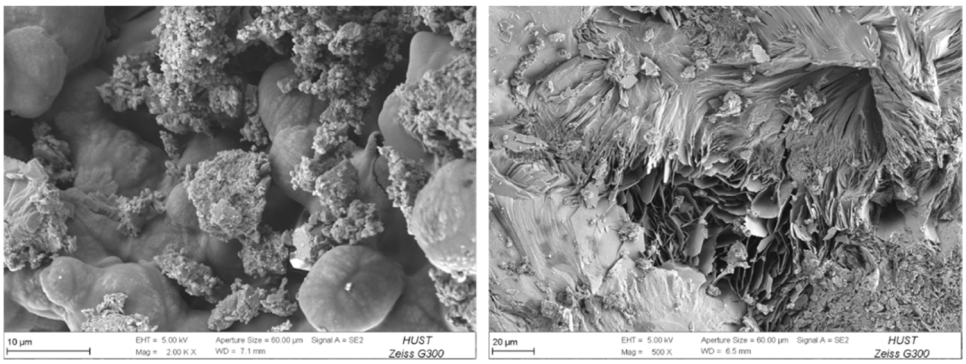

d) EICP(J) + Milk powder and primer

Fig. 15. SEM analyses outcome of EICP(J)s' products in cement paste specimens.

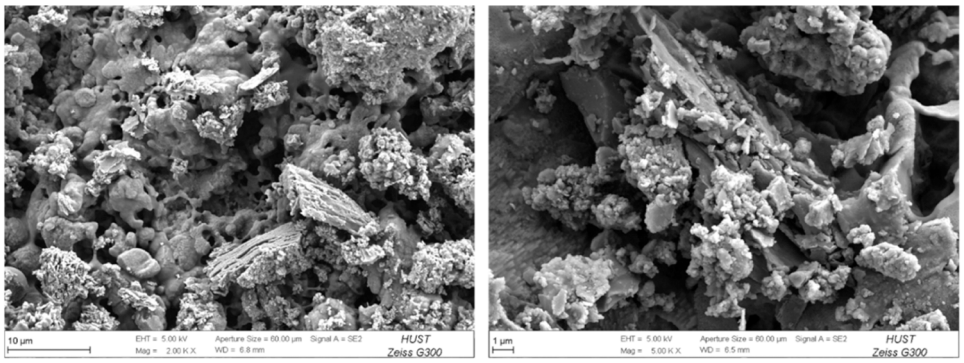

a) EICP(S)

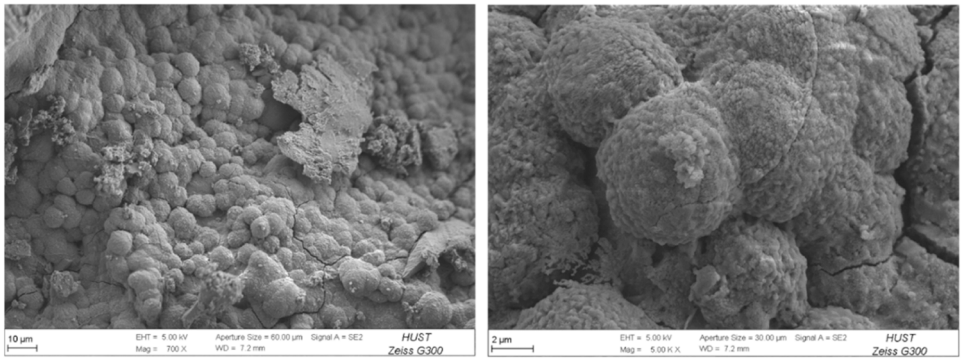

b) EICP(S) + Milk powder

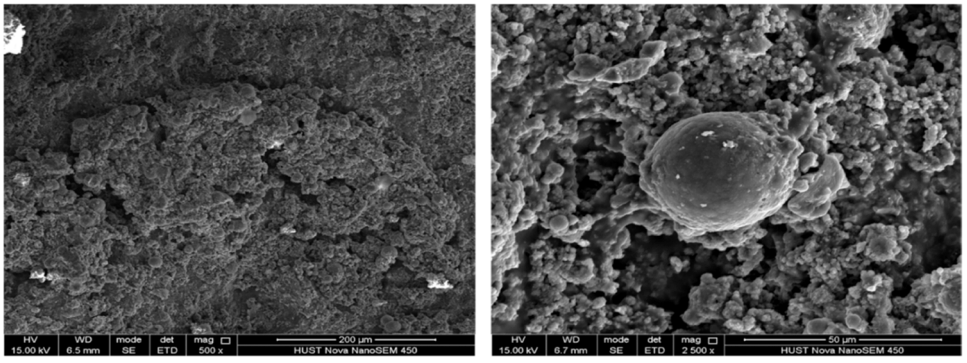

c) EICP(S) + Primer

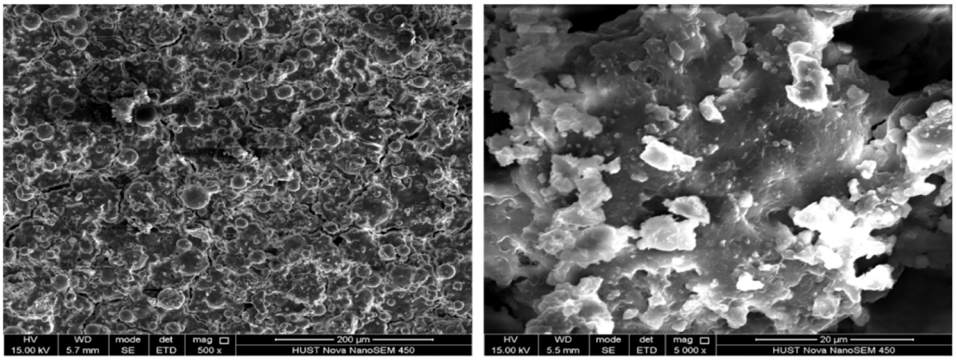

d) EICP(S) + Milk powder and primer

Fig. 16. SEM analyses outcome of EICP(S)s' products in cement paste specimens.

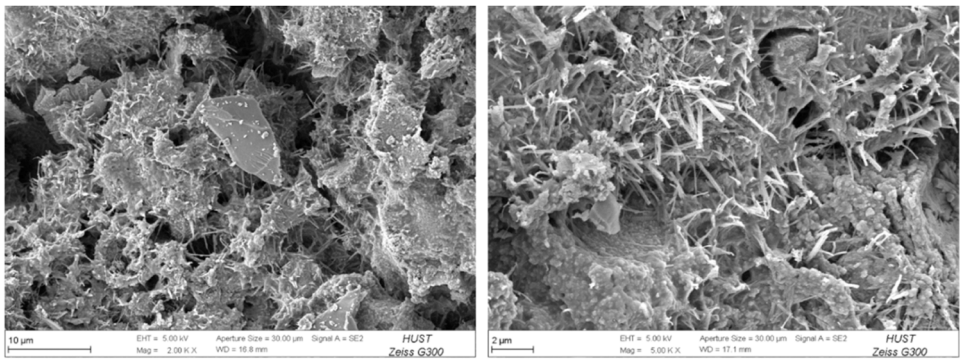

a) MICP

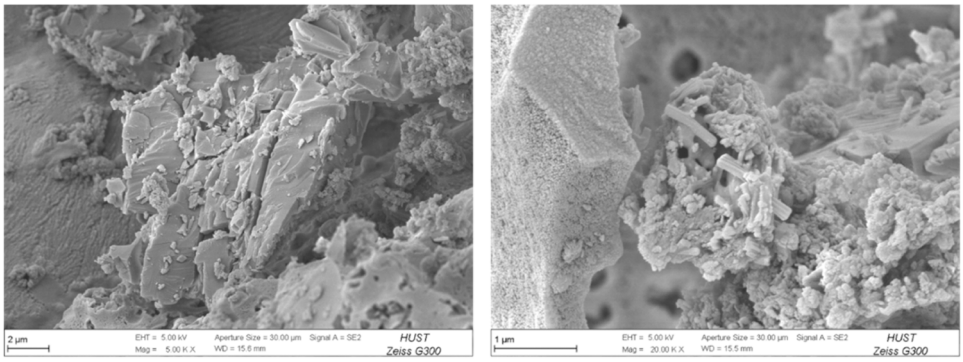

b) MICP + Milk powder

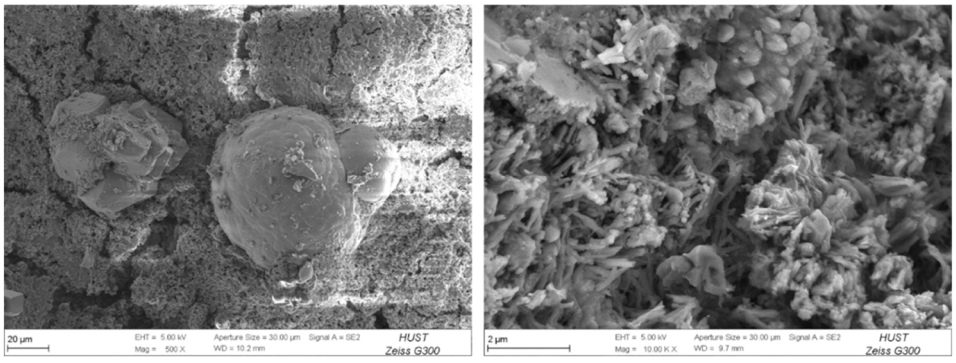

c) MICP + Primer

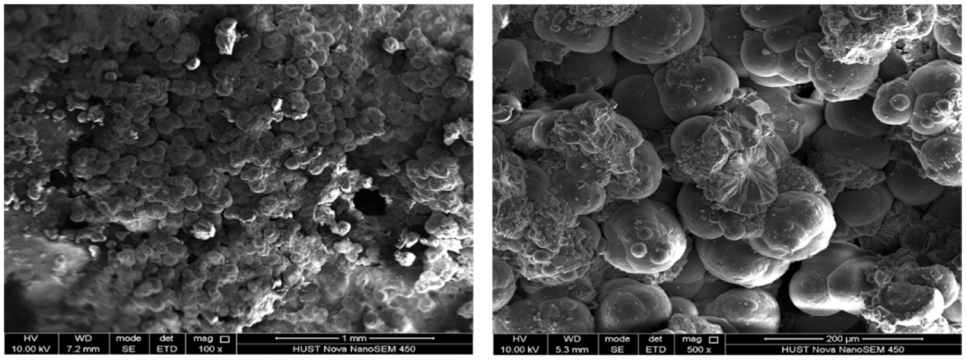

d) MICP + Milk powder and primer

Fig. 17. SEM analyses outcome of MICPs' products in cement mortar specimens.

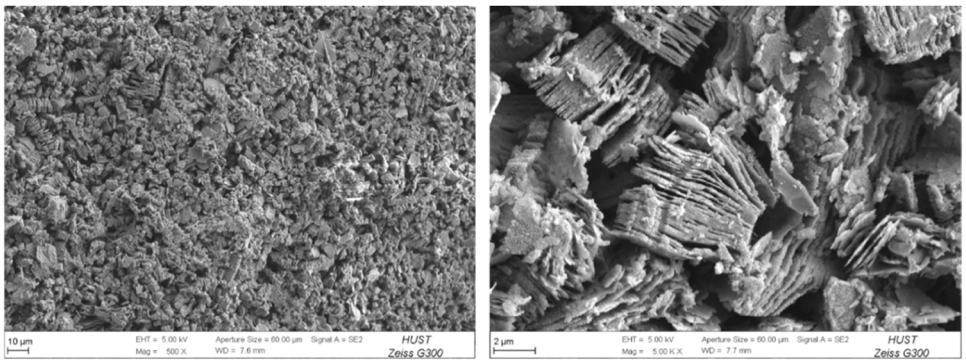

a) EICP(J)

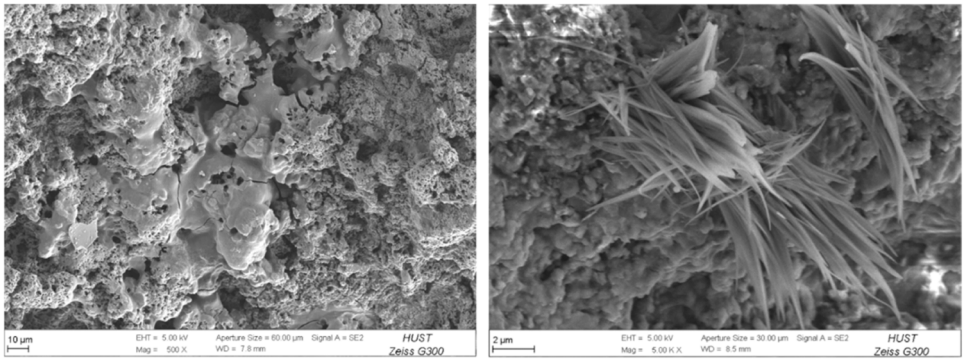

b) EICP(J) + Milk powder

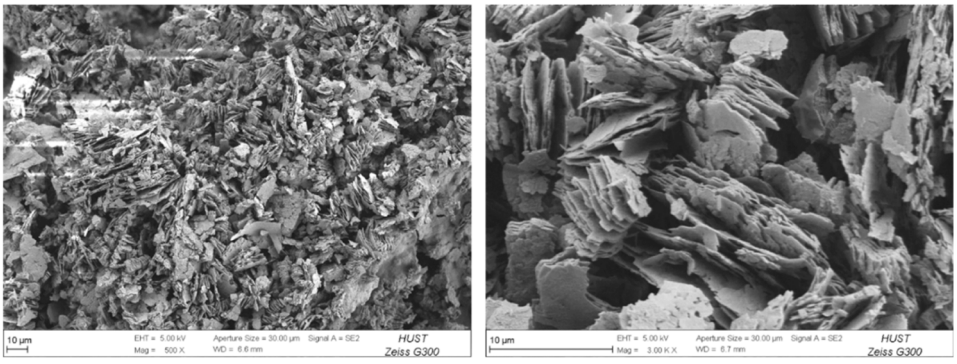

c) EICP(J) + Primer

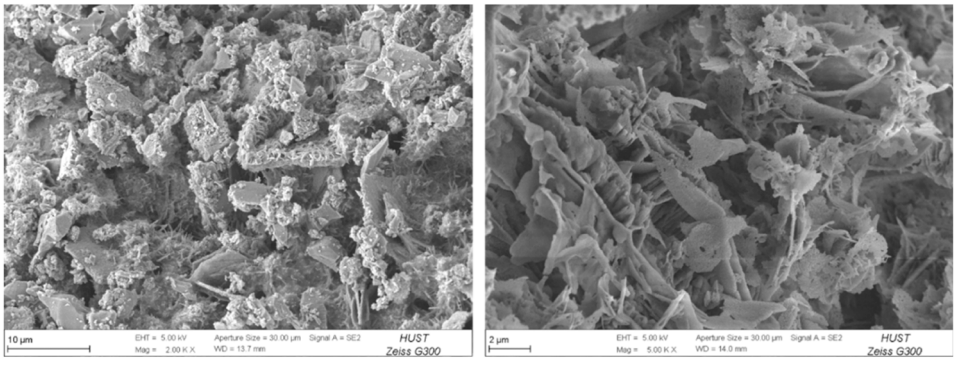

d) EICP(J) + Milk powder and primer

Fig. 18. SEM analyses outcome of EICP(J)s' products in cement mortar specimens.

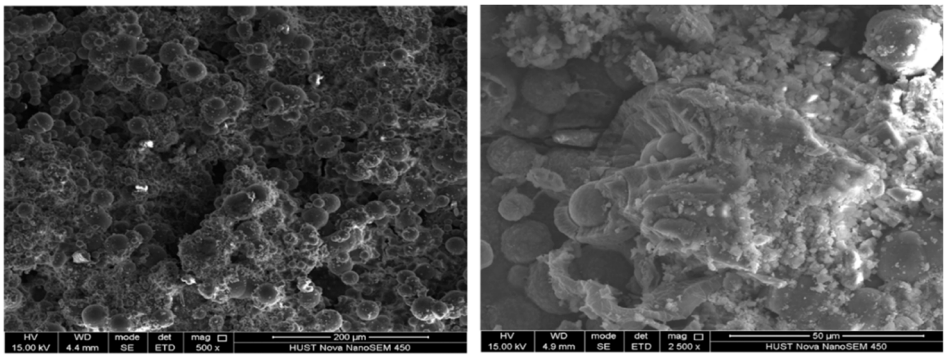

a) EICP(S)

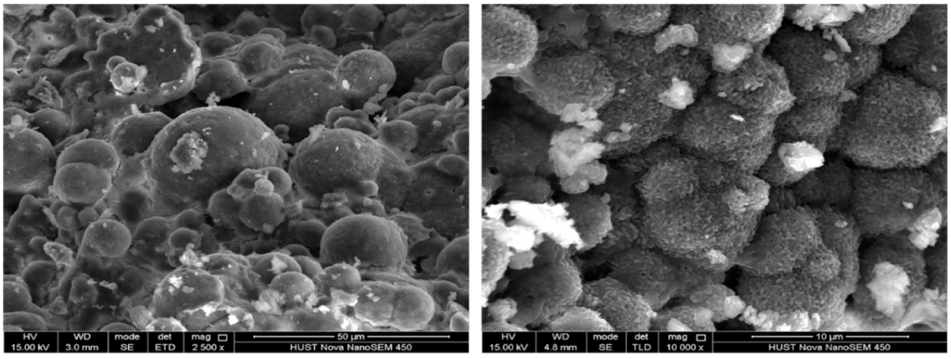

b) EICP(S) + Milk powder

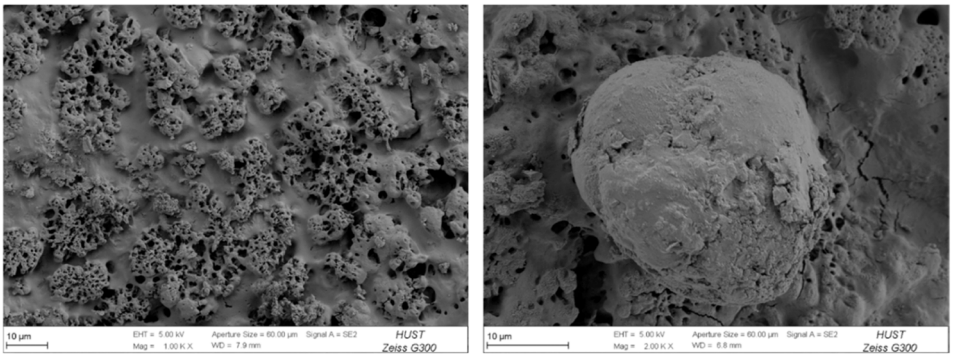

c) EICP(S) + Primer

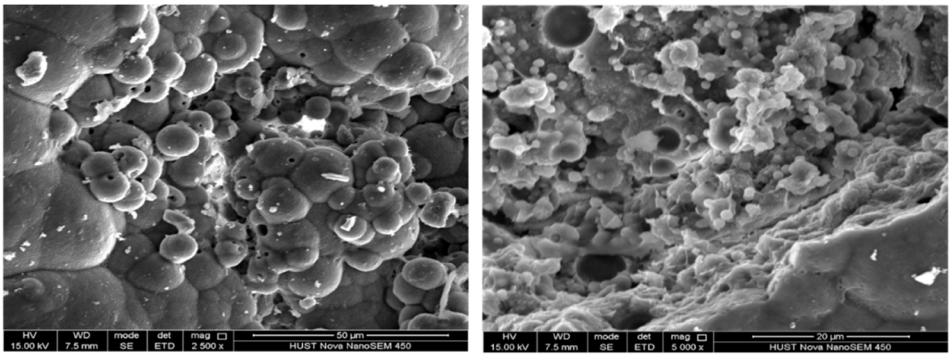

d) EICP(S) + Milk powder and primer

Fig. 19. SEM analyses outcome of EICP(S)s' products in cement mortar specimens.

prior to MICP treatment, the calcium carbonate forms rod-like structures that align longitudinally. These rod-like crystals are more organized and compact, with a rough surface texture due to smaller granular formations adhering to the primary structures (Fig. 14c). The primer appears to influence both the orientation and growth of the crystals. The combination of milk powder and primer with MICP results in the most complex and densely packed crystal structures (Fig. 14d). The calcium carbonate forms layered, fan-shaped, and jagged calcite structures, creating a tightly interwoven network that reflects the synergistic effects between milk powder and primer. This morphology suggests a highly effective crack-filling potential, combining the structural benefits of different MICP approaches.

The calcium carbonate precipitated by EICP(J), without any additives, primarily forms porous, sponge-like structures with irregularly shaped cavities (Fig. 15a). This amorphous, irregular morphology suggests a less organized crystallization process compared to MICP, potentially leading to incomplete crack healing due to the less dense and less structured deposition of calcium carbonate. The addition of milk powder significantly alters the morphology, resulting in highly ordered, elongated structures with a more fibrous and lamellar-like appearance (Fig. 15b). The crystal arrangement becomes more compact and interwoven, indicating a stronger and denser matrix within the crack. The organic components of the milk powder contribute to a more cohesive and structured precipitation process, leading to improved nucleation and growth. In specimens where a primer was applied before EICP(J), calcium carbonate precipitation results in a combination of compact, clustered formations and elongated, fan-shaped structures with the granular particles (Fig. 15c). The primer enhances crystal growth by influencing the orientation and density of the precipitate. The compact, clustered areas contribute to increased surface roughness, potentially improving the mechanical properties of the crack fill. The combination of milk powder and primer yields the most complex and intricate calcium carbonate precipitate structures. The SEM images reveal a mix of rounded, globular formations and fan-like, elongated structures, creating a densely packed, interwoven crystal network (Fig. 15d).

Specimens treated with EICP(S) without additives display calcium carbonate deposits with a loose and irregular granular structure (Fig. 16a). These precipitates lack clear organization, consisting of dispersed and small crystal formations. The absence of well-defined shapes or cohesive structures indicates inefficient crystal growth, which could lead to poor crack-filling capacity. As seen in previous cases, milk powder significantly transforms the crystal morphology of EICP(S) products. The calcium carbonate deposits now feature spherical and globular crystals, in some areas there are visible spherical clusters having smaller as well as larger individual spheres sizes (Fig. 16b). Milk powder appears to foster more organized and denser precipitation, improving the overall distribution of the crystals across the crack, indicative of better crack-filling potential. For specimens with an applied primer, calcium carbonate precipitation exhibits a compact, granular structure with well-adhered formations (Fig. 16c). The crystals are more uniformly distributed than in the conventional sample, and the primer seems to promote more consistent and continuous deposition along the crack. The surfaces show fewer voids and gaps. The combination of granular structures and larger formations provides a smoother surface. In the specimens treated with both milk powder and primer, calcium carbonate precipitation shows the most cohesive and interconnected crystal morphology (Fig. 16d). The calcium carbonate forms dense clusters of spherical crystals, which are tightly packed, creating a uniform layer across the crack surface. This dense and continuous network of crystals maximizes the potential for sealing and reinforcing the crack.

4.3.2. Calcium carbonate in cement mortar specimens

In the conventional MICP treatment, calcium carbonate precipitates display a mix of irregular, clustered, and needle-like crystals (Fig. 17a). The crystal formations are somewhat disorganized, and the surface coverage is sparse, with visible gaps between the deposits. This morphology suggests inefficient crack filling, as the precipitation appears scattered across the surface. The overall loose structure indicates limited adhesion and coverage, making it less effective for complete crack sealing. The incorporation of milk powder induces a distinct transformation in the morphology of calcium carbonate crystals (Fig. 17b). The precipitates become as elongated, rod-like structures prevalent across the surface. In some regions, these crystals form complex, interwoven patterns that contribute to improved surface coverage and cohesion of the deposit. In the MICP with primer treatment, calcium carbonate precipitates are more compact and exhibit a granular structure with a rough, continuous surface (Fig. 17c). The primer treatment seems to promote more organized crystal growth, resulting in fewer gaps and voids in the deposit compared to the conventional MICP treatment. The resulting layer appears more homogeneous, with some areas showing a fine, rough texture that indicates improved adhesion to the crack surface. In the specimens treated with MICP combined with milk powder and primer, the surface is covered with large, spherical crystals that are tightly interwoven to form a thick, cohesive layer.

The calcium carbonate crystals precipitated via EICP(J) treatment predominantly appear as irregular, granular clusters (Fig. 18a). These formations cover the surface relatively uniformly, though the crystals themselves lack distinct shapes, resulting in a somewhat rough texture across the treated crack surface. This suggests a less organized crystallization process, leading to a random distribution of nucleation sites. The introduction of milk powder shifts the crystal morphology, producing a twofold structure (Fig. 18b). The precipitated calcium carbonate fills voids in the cracks, creating irregular, dense shapes with many pores, while also forming elongated fibers or needles on these previously described elements. This variation in morphology is highly dependent on the internal shape of the crack and the underlying structure of its surface, such as the arrangement of sand and pores. When the crack surface is pre-treated with a concrete primer, the calcium carbonate precipitates show a layered, sheet-like morphology (Fig. 18c). These crystalline layers are tightly stacked, providing more comprehensive surface coverage. The primer appears to encourage a more systematic arrangement of the crystals, potentially leading to a stronger bond between the precipitate and the cement matrix. Finally, the combination of milk powder and primer produces the most complex and chaotic crystal structures among the EICP(J)-treated specimens. The calcium carbonate forms elongated, plate-like crystals that fan out in intricate patterns, combining the crystal shapes observed in previous treatments (Fig. 18d). These formations are densely packed and interlocked, which could be beneficial in terms of mechanical strength.

The calcium carbonate crystals precipitated by conventional EICP(S) treatment exhibit a predominantly spherical morphology, forming compact clusters across the crack surface. These spherical crystals appear densely packed, with minimal voids between them (Fig. 19a). The uniformity in crystal shape suggests a consistent nucleation process, resulting in relatively even coverage of the crack surface. However, the spherical form may limit the extent of crack filling due to potential gaps between the crystals. In the EICP(S) treatment with milk powder, there is not a significant change in crystal morphology compared to the other cases. The calcium carbonate crystals maintain a spherical shape but appear larger and more robust (Fig. 19b). The surfaces of these spheres are rougher, and some exhibit a layered structure, indicating more complex crystal growth dynamics. The increased size and roughness of the crystals, combined with their dense packing, suggest enhanced nucleation and growth facilitated by the organic components of the milk powder, potentially improving the sealing efficiency of the treatment. The application of a concrete primer before EICP(S) treatment results in the formation of distinct, irregularly shaped calcium carbonate crystals (Fig. 19c). These crystals are larger and more angular compared to those in untreated (without primer) cracks. The irregular shapes and increased crystal size suggest that the primer influences the crystallization environment. Lastly, the combination of milk powder and primer in the EICP

(S) process produces a complex mixture of morphologies. The calcium carbonate crystals exhibit spherical shapes of different sizes, with some formations appearing as fused clusters (Fig. 19d). This hybrid morphology indicates that the combined effects of milk powder and primer lead to diverse nucleation and growth mechanisms. The resulting crystal structures are densely packed and interlocked, creating a highly textured surface that likely offers superior crack sealing and reinforcement.

4.4. General comparison of EICP and MICP method

EICP and MICP are both promising techniques for applications such as crack repair in cementitious materials or soil improvement. While both rely on calcium carbonate precipitation, they differ significantly in terms of cost-effectiveness, environmental impact, and long-term durability. EICP is generally more cost-effective (i.e., especially used cured plant urease) than MICP due to its simpler process. It uses enzymes like urease, which can be directly added to the treatment solution, eliminating the need for microbial cultivation. Additionally, such urease can be obtained from the leguminous plants, and further reduce the cost. In contrast, MICP requires the growth and maintenance of bacterial cultures, which involves additional infrastructure, time, and resources. This makes EICP more suitable for projects with budget constraints or where rapid deployment is necessary. From an environmental perspective, EICP is often seen as more favorable. Since it avoids the use of live microorganisms, it reduces risks of environmental contamination and biohazard concerns. However, EICP still involves urea hydrolysis, which can release ammonia into the environment, requiring proper management. On the other hand, while MICP can contribute to biogenic aesthetics and natural integration, it involves live bacteria, posing challenges such as waste management and regulatory compliance. Considering the long-term durability, MICP holds a distinct advantage. The presence of bacteria in the system can potentially sustain precipitation of calcium carbonate under favorable conditions, prolonging the effectiveness of the repair or stabilization. EICP, while capable of rapid and effective precipitation, lacks the self-sustaining capability provided by microbial activity, which might limit its performance over extended periods.

Overall, EICP is advantageous for its cost efficiency, simplicity, rapid implementation, and reduced biohazard concerns, making it ideal for applications requiring quick and economical solutions. However, it may lack the long-term self-healing capabilities associated with MICP. Conversely, MICP offers potential benefits in prolonged durability and self-sustainability, making it more suitable for projects where these factors are a priority, despite its higher costs and more complex operational requirements. A careful assessment of project needs is essential to determine the most appropriate method.

5. Conclusions

In conclusion, this study systematically evaluated the efficacy of Enzyme-Induced Carbonate Precipitation and Microbially Induced Calcium Carbonate Precipitation for repairing external cracks in cement-based materials. The research provides valuable insights into the morphological, chemical, and crystallographic characteristics of the calcium carbonate precipitates formed by these bio-mediated techniques. The following conclusions can be drawn from the study:

1. Both EICPs and MICP demonstrated effectiveness in sealing cracks smaller than 0.35 mm, with calcium carbonate precipitation filling these cracks substantially, covering more than 95 % of the crack surface. However, cracks wider than 0.35 mm showed limited filling capacity, with the coverage of the crack surface being in the range of 15 %-80 %, indicating a threshold beyond which the methods' effectiveness diminishes.
2. MICP treatments predominantly produced calcium carbonate with high purity and uniform crystal structures, primarily calcite with some vaterite presence. In contrast, EICPs-treated samples exhibited a more complex mineralogy, with additional elements like chlorine and sulfur indicating varied crystallization environments, particularly when additives were used. Furthermore, the use of additives (i.e., powder milk and primer), benefits the crystallite size of precipitated calcium carbonate.
3. The introduction of milk powder and primer significantly altered the morphology and crystallization patterns of calcium carbonate in both EICPs and MICP. With the authors' assumptions, these additives likely influenced the precipitation process through their chemical compositions - milk powder, rich in proteins and lactose, potentially acted as nucleation sites, while the water-base epoxy resin primer and its penetrating agents may have provided a more conducive environment for crystal growth. Together, they enhanced crack-filling efficiency by promoting denser, more cohesive crystal formations. The combined use of milk powder and primer produced the most effective crack sealing, resulting in highly interwoven and densely packed crystal networks.
4. SEM analyses revealed distinct differences in the surface morphology of calcium carbonate precipitates between MICP and EICPs treatments. EICPs generally resulted in more organized and densely packed crystal structures, while MICP, particularly with plant-derived urease, produced more irregular morphology and porous formations. The use of additives, as mentioned in point 3, subtly refined these characteristics, guiding the crystallization process toward more cohesive and robust structures across both methods.
5. The study highlights the potential of EICPs and MICPs as sustainable alternatives to traditional crack repair methods in cement-based materials. However, their application may be limited by the crack size. The choice of method and additives should be tailored to the specific requirements of the repair scenario, considering factors like crack width, material composition, and desired durability, which should be further studies.

This research contributes to the growing body of knowledge on bio-related crack repair techniques, offering practical insights for their implementation in civil engineering. Future work could explore the long-term durability and mechanical properties of the repaired materials, developing novel additives to enhance the efficiency and adaptability of EICP and MICP, optimizing their performance across various materials. Investigating their use in complex structures, such as historical buildings, could address unique preservation challenges. Additionally, integrating these techniques with other self-healing technologies may lead to multifunctional materials, advancing sustainable and resilient construction practices.

CRediT authorship contribution statement

M.J. Jedrzejko: Conceptualization, Methodology, Validation, Investigation, Writing – original draft, Visualization, Project administration. **Y. Gan:** Conceptualization, Writing – review & editing, Supervisiona. **H.M. Jonkers:** Writing – review & editing, Supervision. **H. Luo:** Writing – review & editing, Supervision, Funding acquisition.

Declaration of Competing Interest

The authors declare that they have no known competing financial interests or personal relationships that could have appeared to influence the work reported in this paper.

Acknowledgements

The authors are grateful for the financial support received from the National Natural Science Foundation of China (Grant No. 52408261).

Appendix A. Supporting information

Supplementary data associated with this article can be found in the online version at doi:10.1016/j.conbuildmat.2024.139646.

Data availability

Data will be made available on request.

References

[1] A.M. Neville. Properties of Concrete, 5th edition), Pearson Education Limited, Essex, 2011.
[2] F. Pacheco-Torgal, S. Jalali, A. Fucic, UK. Toxicity of Building Materials, Woodhead Publishing, 2012.
[3] P.K. Mehta, P.J.M. Monteiro. Concrete: Microstructure, Properties, and Materials, 4th edition), McGraw-Hill Education, New York, 2014.
[4] M. Kayondo, R. Combrinck, W.P. Boshoff, State-of-the-art review on plastic cracking of concrete, Constr. Build. Mater. 225 (2019) 886–899.
[5] G.L. Golewski, The phenomenon of cracking in cement concretes and reinforced concrete structures: the mechanism of cracks formation, causes of their initiation, types and places of occurrence, and method of detection - a review, Buildings 13 (3) (2023) 765.
[6] C.M. Aldea, S.P. Shah, A. Karr, Effect of cracking on water and chloride permeability of concrete, Mater. Civ. Eng. 11 (3) (1999).
[7] W.A. Thanoon, M.S. Jaafar, M. Razali, A. Kadir, J. Noorzaei, Repair and structural performance of initially cracked slabs, Constr. Build. Mater. 19 (8) (2005) 595–603.
[8] R. Francois, S. Laurens, F. Deby, Corrosion and its consequences for reinforced concrete structures, ISTE Press and Elsevier, UK and USA, 2018.
[9] F.U.A. Shaikh, Effect of cracking on corrosion of steel in concrete, Int. J. Concr. Struct. Mater. 12 (3) (2018).
[10] N. Delatte, Failure, distress and repair of concrete structures, Woodhead publishing in materials, 2009.
[11] T.K. Kim, J.S. Park, Performance evaluation of concrete structures using crack repair methods, Sustainabillity 13 (6) (2021) 3217.
[12] C.A. Issa, P. Debs, Experimental study of epoxy repairing of cracks in concrete, Constr. Build. Mater. 21 (1) (2007) 157–163.
[13] T.K. Kim, J.S. Park, Performance evaluation of concrete structures using crack repair methods, Sustainability 13 (6) (2021) 3217.
[14] M.A. Safan, Z.A. Etman, A. Konswa, Evaluation of polyurethane resin injection for concrete leak repair, Case Stud. Constr. Mater. 11 (2019) e00307.
[15] H.M.C.C. Somarathan, S.N. Raman, D. Mohotti, A.A. Mutalib, K.H. Badri, The use of polyurethane for structural and infrastructural engineering applications: a state-of-the-art review, Constr. Build. Mater. 190 (2018) 995–1014.
[16] Song X., Song X., Liu H., Huang H., Anvarovna K.G., Ugli N.A.D., Huang Y., Hu J., Wei J. and Yu Q. Cement-based repair materials and the interface with concrete substrates: Characterization, evaluation and improvement. Polymers 1022, 14(7), 1485.
[17] R. Goushis, K.M. Mini, Effectivness of polymeric and cementitious materials to secure crack in concrete under diverse circumstances, Int. J. Adhes. Adhes. 114 (2022) 103099.
[18] L.W. ElKhatib, A. Elkordi, J. Khatib, Methods and surface materials repair for concrete structures – a review, BAU J. Sci. Technol. 4 (2) (2023) 7.
[19] Z.J. He, X.D. Zhu, J.J. Wnag, M. Mu, Y. Wang, Comparison of CO_2 emission from OPC and recycled cement production, Constr. Build. Mater. 211 (30) (2019) 965–973.
[20] S. Nie, J. Zhou, F. Yang, M.Z. Lan, J.M. Li, Z.Q. Zhang, Z.F. Chen, M.F. Xu, H. Li, J. G. Sanjayan, Analysis of theoretical carbon dioxide emissions from cement production: methodology and application, J. Clean. Prod. 334 (2022) 130270.
[21] M. Seifan, A. Berenjian, Microbially induced calcium carbonate precipitation: a widespread phenomenon in the biological world, Appl. Microbiol. Biotechnol. 103 (2019) 4693–4708.
[22] M.J. Castro-Alonso, L.E. Montanez-Hernandez, M.A. Sanchez-Munoz, M.R. Macias Franco, R. Narayanasamy, N. Balagurusamy, Microbially induced calcium carbonate precipitation (MICP) and its potential in bioconcrete: microbiological and molecular concepts, Front. Mater. 6 (2019) 126.
[23] Y. Liu, A. Amjad, J.F. Su, K. Li, R.Z. Hu, Z. Wang, Microbial-induced calcium carbonate precipitation: influencing factors, nucleation pathways, and application in waste water remediation, Sci. Total Environ. 860 (2023) 160439.
[24] I. Ahenkorah, M. Rahman, R. Karim, S. Beecham, C. Saint, A review of enzyme induced carbonate precipitation (EICP): the role of enzyme kinetics, Sustain. Chem. 2 (1) (2021) 92–114.
[25] W. Hu, W.C. Cheng, S. Wen, K. Yuan, Revealing the enhancement and degradation mechanism affecting the performance of carbonate precipitation in EICP process, Front. Bioeng. Biotechnol. 9 (2021) 750258.
[26] R. Ligabue-Braun, C.R. Carlini, Urease - Functions. Classes, and Applications, 1st edition), Academic press, 2024.
[27] M. Weber, M.J. Jones, J. Ulrich, Optimisation of isolation and purification of the jack bean enzyme urease by extraction and subsequent crystallization, Food Bioprod. Process. 86 (1) (2008) 43–52.
[28] B. Krajewska, Urease I. Functional, catalytic and kinetic properties: a review, J. Mol. Catal. B: Enzym. 59 (1-3) (2009) 9–21.
[29] S. Kumar, A.M. Kayastha, Soybean (Glycine max) urease: significance of sulfhydryl groups in urea catalysis, Plant Physiol. Biochem. 15 (9) (2010) 746–750.
[30] H.K. Tirkolaei, N. Javadi, V. Krishnan, N. Hamdan, E. Kavazanjian Jr., Crude urease extract for biocementation, J. Mater. Civ. Eng. 32 (12) (2020) 04020374.
[31] I. Ahenkorah, M.M. Rahman, M.R. And Karim, S. Beecham, Enzyme induced calcium carbonate precipitation and its engineering application: a systematic review and meta-analysis, Constr. Build. Mater. 308 (2021) 125000.
[32] M.J. Cui, H.J. Lai, S.F. Wu, J. Chu, Comparison of soil improvement methods using crude soybean enzyme, bacterial enzyme or bacteria-induced carbonate precipitation, Geotechnique 74 (1) (2022) 18–26.
[33] H.J. Lai, M.J. Cui, S.F. Wu, Y. Yang, J. Chu, Extraction of cured soybean urease using ethanol and its effect on soil cementation, Soil Found. 63 (2023) 101300.
[34] Y. Liu, Y.F. Gao, Y.D. Zhou, H. Meng, C. Li, Evaluation of enzyme-induced carbonate precipitation using crude soybean urease during soil percolation, Acta Geotech. 19 (2024) 1571–1580.
[35] L.X. Liu, Y.F. Gao, W.J. Geng, J. Song, Y.D. Zhou, C. Li, Comparison of jack bean and soybean cured ureases on surface stabilization of desert sand via enzyme-induced carbonate precipitation, Geoderma 435 (2023) 116504.
[36] M.Y. Wu, X.M. Hu, Q. Zhang, Y.Y. Zhao, J.H. Sun, W.M. Cheng, Y.J. Fan, S.C. Zhu, W. Lu, C.Y. Song, Preparation and performance evaluation of environment-friendly biological dust suppressant, J. Clean. Prod. 273 (2020) 123162.
[37] D. Mujah, M.A. Shahin, L. Cheng, State-of-the-art review of biocementation by microbially induced calcite precipitation (MICP) for soil stabilization, Geomicrobiol. J. 34 (6) (2017) 524–537.
[38] C.S. Tang, L.Y. Yin, N.J. Jiang, C. Zhu, H. Zheng, H. Li, B. Shi, Factors affecting the performance of microbial-induced carbonate precipitation (MICP) treated soil: a review, Environ. Earth Sci. 79 (94) (2020).
[39] Y.Q. Chen, S.Q. Wang, X.Y. Tong, X. Kang, Crystal transformation and self-assembly theory of microbially induced calcium carbonate precipitation, Appl. Microbiol. Biotechnol. 106 (2022) 3555–3569.
[40] Y.Q. Chen, S.Q. Wang, X.Y. Tong, X. Kang, Towards the sustainable fine control of microbially induced calcium carbonate precipitation, J. Clean. Prod. 377 (2022) 134395.
[41] S.Q. Wang, Y.Q. Chen, R.P. Chen, X.Y. Ma, X. Kang, Steerable artificial magnetic bacteria with target delivery ablility of calcium carbonate for soil improvement, Appl. Microbiol. Biotechnol. 107 (2023) 5687–5700.
[42] H.M. Jonkers, A. Thijssen, G. Muyzer, O. Copuroglu, E. Schlangen, Application of bacteria as self-healing agent for the development of sustainable concrete, Ecol. Eng. 36 (2) (2010) 230–235.
[43] V. Wiktor, H.M. Jonkers, Quantification of crack-healing in novel bacteria-based self-healing concrete, Cem. Concr. Compos. 33 (7) (2011) 763–770.
[44] R. Davies, O. Teall, M. Pilegis, A. Kanellopoulos, T. Sharma, A. Jefferson, D. Gardner, A. Al-Tabbaa, K. Paine, R. Lark, Large scale application of self-healing concrete: design, construction and testing, Front. Mater. 5 (2018) 51.
[45] M. Amran, A.M. Onaizi, R. Fediuk, N.I. Vatin, R.S.M. Rashid, H. Abdelgader, T. Ozbakkaloglu, Self-healing concrete as a prospective construction material: a review, Materials 15 (9) (2022) 3214.
[46] P. Jongvivatsakul, K. Janprasit, P. Nuaklong, W. Pungrasmi, S. Likitlersuang, Investigation of the crack healing performance in mortar using microbially induced calcium carbonate precipitation (MICP) method, Constr. Build. Mater. 212 (2019) 737–744.
[47] X. Sun, L. Miao, Application of Bio-remedition with Bacillus megaterium for crack repair at low temperature, J. Adv. Concr. Technol. 18 (2020) 307–319.
[48] R. Gao, J. Ma, G. Liu, H. Chen, J. Wen, J. Wang, Optimization of deposition process for a productive and cohesive bio-$CaCO_3$ to repair concrete existing cracks, Appl. Microbiol. Biotechnol. 107 (2023) 3479–3494.
[49] R. Junwale, A. Nikode, S. Bhutange, M.V. Latkar, Crack healing in cement mortar using enzyme induced calcium carbonate precipitation, Constr. Build. Mater. 394 (2023) 132223.
[50] H. Yuan, M. Ru, W. Dong, X. Zhu, Z. Zhao, Crack repair in in-service tunnel linings using chitosan-combined enzyme-induced carbonate precipitation, J. Mater. Civ. Eng. 36 (11) (2024) 04024365.
[51] G. Li, D. Yan, J. Liu, P. Yang, J. Zhang, Experimental study on the crack concrete repaired via enzyme-induced calcium carbonate precipitation (EICP), Materials 17 (13) (2024) 3205.
[52] M.G. Arab, R. Alsodi, A. Almajed, H. Yasuhara, W. Zeiada, M.A. Shahin, State-of-the-art review of enzyme-induced calcite precipitation (EICP) for ground improvement: applications and prospects, Geosciences 11 (12) (2021) 492.
[53] A. Almajed, H.K. Tirkolaei, E. Kavazanjian Jr., N. Hamdan, Enzyme induced biocementated sand with high strength at low carbonate content, Geosciences 11 (12) (2021) 492.